Journal of Structural Geology 202 (2026) 105564

Contents lists available at ScienceDirect

Journal of Structural Geology

journal homepage: www.elsevier.com/locate/jsg

What do flexural normal faults tell us about fold-and-thrust belts and foredeep flexures? Cantabrian zone (Ibero-Armorican Orocline core) examples

Mayte Bulnes [a], Hodei Uzkeda [b], Josep Poblet [a,*], Iván García Zuazua [c]

[a] Departamento de Geología, Universidad de Oviedo, C/Jesús Arias de Velasco s/n, Oviedo, 33005, Spain
[b] Departamento de Geodinámica, Estratigrafía y Paleontología, Universidad Complutense de Madrid, C/ de José Antonio Novais 12, Madrid, 28040, Spain
[c] Cemosa, Urbanización Monsagre, Nave 7, Carretera de Viella, Siero, 33429, Spain

ARTICLE INFO

Keywords:
Flexural normal fault
Fold-and-thrust belt
Foredeep flexure
Thrust propagation sequence
Oblique/lateral structure
Cantabrian zone

ABSTRACT

This work describes how flexural normal faults related to a flexure produced in the foredeep of a fold-and-thrust belt develop, how they can be recognized, especially when they formed in early or intermediate stages of development of the fold-and-thrust belt, what information provide about the fold-and-thrust belt and the foredeep flexure, and different procedures to obtain it. The application of these methodologies to a natural example is shown through the detailed analysis of normal faults preceding the folds and thrusts in the western part of the Cantabrian Zone, the foreland fold-and-thrust belt of the Variscan Orogen in the northwest portion of the Iberian Peninsula. These faults are interpreted as flexural normal faults formed during the fold-and-thrust belt development. The strike of the longitudinal flexural normal faults illustrates the orientation of the old fold-and-thrust belt front, resulting in an arcuate distribution consistent with the geometry of the Ibero-Armorican or Asturian Arc. The low fracturing intensity due to the longitudinal faults indicates that the flexure curvature and the flexure inclined-limb dip were very gentle, and that the flexure interlimb angle was very high. This may suggest that the fold-and-thrust belt weight was low at that time. The timing of these flexural normal faults indicate that the thrusts propagated following a forward-breaking or "piggy-back" sequence, as deduced by other authors employing different methods. Finally, the transverse flexural normal faults are interpreted as a result of large oblique/lateral thrust ramps in some thrust sheets located in the southern part of the Cantabrian Zone.

1. Introduction

Structural style is defined as the set of characteristic features and patterns displayed by geological structures within a given region, formed under a common tectonic regime. Each structural style comprises an association of structures that developed broadly contemporaneously, although in some cases local, mutual cross-cutting relationships indicate that certain structures predate or postdate others. Well-documented examples of such relationships are now available in the literature (e.g., Gray, 1981; Lacombe and Beaudoin, 2024).

One of the benefits of discovering that different types of structures formed during the same event is that once this relationship is established, the study of the features of one type of structure supplies further information about the other type of structure. For example, in a restraining bend of a major strike-slip fault, a push-up ridge may develop formed by reverse faults and folds (e.g., Smith et al., 2007; Mitra and Paul, 2011). A measure of the amount of shortening responsible for the formation of reverse faults and folds provides the amount of strike separation of the main strike-slip fault. In the case of rollover anticlines related to listric normal faults (e.g., McNeill et al., 1997; Poblet and Bulnes, 2005), the rollover indicates that the fault responsible for its formation is listric and vice versa. Moreover, the application of a series of specific graphical techniques employing the rollover morphology allows obtaining the normal fault geometry at depth accurately (e.g., Verrall, 1981; Davison, 1986; White et al., 1986; Williams and Vann, 1987) or, it is also possible to reconstruct the geometry of the rollover located in the fault hangingwall based on the normal fault shape (e.g., White et al., 1986; Moretti et al., 1988; Groshong Jr, 1989; Waltham,

This article is part of a special issue entitled: Richard Lisle published in Journal of Structural Geology.

* Corresponding author.
E-mail addresses: maite@uniovi.es (M. Bulnes), huzkeda@ucm.es (H. Uzkeda), jpoblet@uniovi.es (J. Poblet), ivangarzu@gmail.com (I. García Zuazua).

https://doi.org/10.1016/j.jsg.2025.105564
Received 10 August 2025; Received in revised form 10 October 2025; Accepted 20 October 2025
Available online 21 October 2025

1989). Similarly, in the case of folds developed in the hangingwall of thrust ramps (e.g., Boyer, 1986; Rodríguez et al., 2021), a set of techniques has been developed to reconstruct the geometry of the thrust at depth based on the fold morphology, or vice versa, i.e., to reconstruct the geometry of the hangingwall fold based on the thrust shape (e.g., Geiser et al., 1988; Suppe, 1983; Mary, 1983; Mitra and Paul, 2011; Suppe and Medwedeff, 1990).

However, before obtaining this information, one must determine whether the different types of structures originated during the same deformational event through a careful structural analysis, paying attention to aspects such as those listed below. One of them is the relative location of the structures. For instance, diapirs, anticlines, and normal faults coexist (e.g., Davison et al., 2000; Rodríguez et al., 2022c) but they are not randomly distributed. The cores of the anticlines are typically pierced by evaporites or mudstones, while minor normal faults are preferentially located in the diapir crests. The size and frequency of the structures may be also important. For example, the normal faults developed in the foredeep flexures caused by fold-and-thrust belts (e.g., Chou and Yu, 2002; Rodríguez et al., 2022a) are usually smaller and sparser than the thrusts. The strike and dip of the structures may be useful elements as well. For instance, in a fault-propagation fold related to a dip-slip normal fault (e.g., Sharp et al., 2000; Khalil and McClay, 2002), the inclined limb located between the monoclinal hinges strikes and dips in the same directions as the normal fault. Another key aspect may be the sense of motion of the structures. For example, the small reverse faults developed in the hangingwall of a ramp-flat listric normal fault (e.g., McClay, 1990, 1996), exhibit a motion sense equal to that of the main normal fault. The amount of horizontal motion caused by the structures may be an essential element as well. For instance, normal faults form in the rear part of a toe thrust, while thrusts develop in the frontal part (e.g., Worrall and Snelson, 1989; Cobbold et al., 1995). The normal-faulting related extension should be roughly equivalent to the thrusting related shortening. Additionally, the compatibility of the stress fields responsible for different types of structures may be a critical factor. For example, the normal faults in pull-apart basins formed in releasing bends along major strike-slip faults (e.g., Freund, 1971; McClay and Dooley, 1995) should be compatible with the stress field inferred from the strike-slip faults. Another parameter may be the relative timing of the structures. For instance, the gravitational normal faults developed in the crest and limbs of an anticline (e.g., Muñoz et al., 1994; Pace et al., 2017; Rodríguez et al., 2022b) cut through inclined layers in their footwall, indicating that the faults developed after the anticline amplification onset.

In this article we deal with different types of structures: normal faults, thrusts, and folds. Specifically, we focus on flexural normal faults related to a foredeep flexure in front of a fold-and-thrust belt (Fig. 1). The purpose of our work is to determine what the study of flexural normal faults can contribute beyond their own characterization with respect to the foredeep flexure and the fold-and-thrust belt. However, to achieve this, it is first necessary to be able to recognize that the normal faults are flexural normal faults developed during the same deformational event as the folds and thrusts.

To this end, the first part of this article is a theoretical approach aiming to supply criteria to be used to distinguish flexural normal faults from other types of normal faults, based on analysing how these faults form. Next, a series of techniques are designed to obtain information about the foredeep and the contractional belt based on the study of flexural normal faults. In the second part of the article, the diagnostic criteria for flexural normal faults are applied to a field example for which a detailed structural analysis has been conducted, and the previously designed techniques are implemented. Many studies conducted so far on this topic (e.g., Bradley and Kidd, 1991; Doglioni, 1995; Chou and Yu, 2002) have been devoted to the flexural extension of the upper continental crust in contractional foredeeps due to bending, i.e., at a large scale. Moreover, these studies have primarily considered foredeeps located in front of fold-and-thrust belts, affected only by a flexure and normal faults, i.e., flexures and flexural normal faults formed in the final stages of fold-and-thrust belt development (Fig. 1). However, our study examines small-scale flexural normal faults and deals with faults not only developed in the final stages but also with those developed in the early or intermediate stages of fold-and-thrust belt evolution. As a result, the former foredeeps, along with their flexure and flexural normal faults, are now located within different thrust sheets and interact with contractional structures (Fig. 2a).

The specific goals pursued in the theoretical part of this article are briefly outlined below.

i) Identify the main mechanisms responsible for the amplification of foredeep flexures and generation of related longitudinal normal faults.
ii) Describe different criteria for recognizing longitudinal flexural normal faults, especially when they develop in early or intermediate stages of a fold-and-thrust belt and become incorporated into various thrust sheets.
iii) Provide different strategies to be employed for gathering different types of data about fold-and-thrust belts and foredeep flexures through the analysis of longitudinal flexural normal faults.
iv) Describe the main causes responsible for the development of transverse flexural normal faults, and list diagnostic criteria to identify them especially when they develop in early or intermediate stages of a fold-and-thrust belt.
v) Warn that the restoration of geological sections across thrusts and related folds in contexts similar to the one studied here must take into account the pre-contractional structure of the layers.

The chosen natural example to check these methodologies is the western part of the Cantabrian Zone (Fig. 3). The Cantabrian Zone, located in the core of the Ibero-Armorican or Asturian Arc (e.g., Suess, 1892; Lotze, 1945), is the foreland fold-and-thrust belt of the Variscan

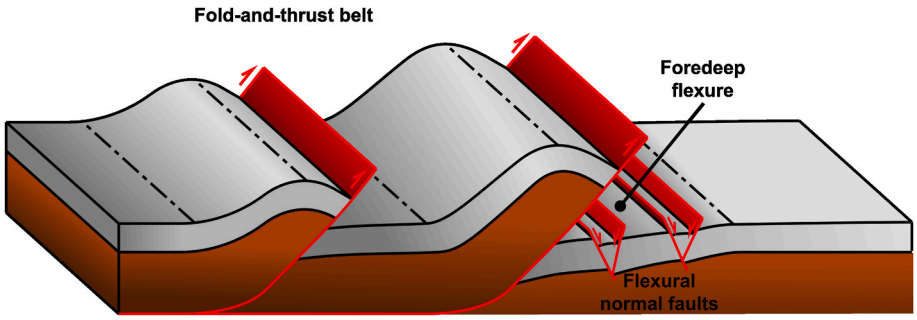

Fig. 1. Idealized schematic block diagram showing a foredeep flexure and associated longitudinal flexural normal faults in front of a fold-and-thrust belt. The dashed-dotted lines are the axial traces of the folds. The dips of the layers and faults, as well as the angles between them, do not represent actual values, but have been used to better visualize the figure.

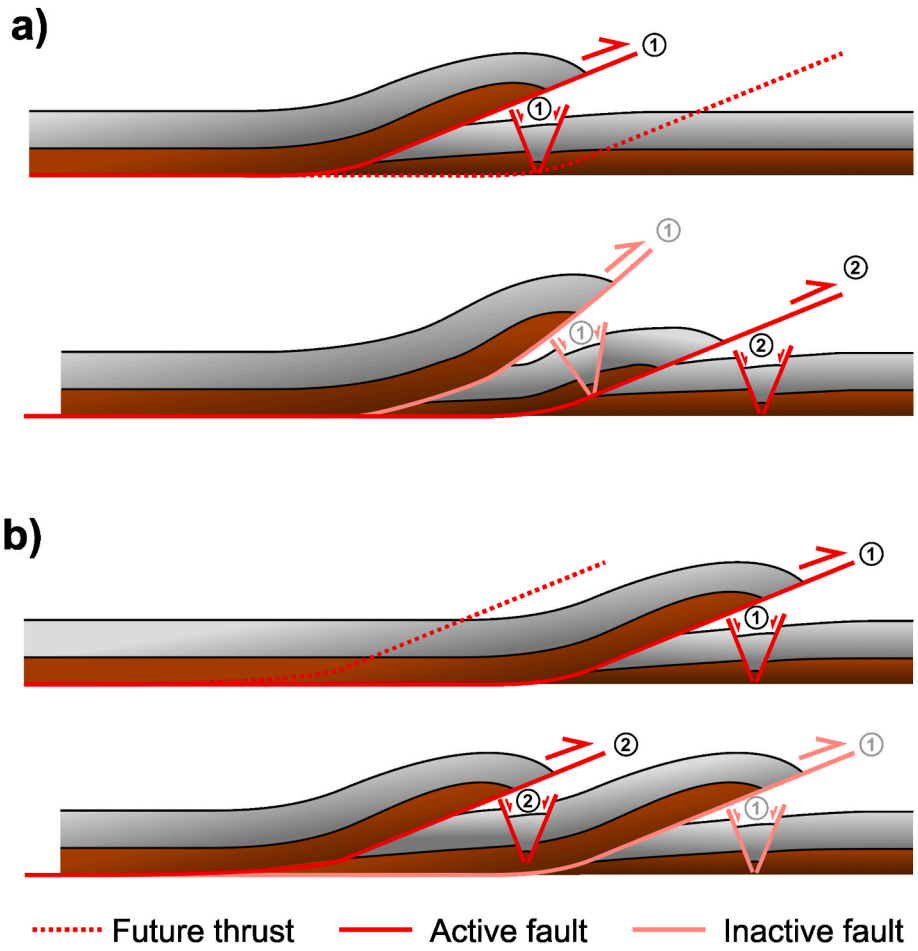

Fig. 2. Idealized schematic cross-sections showing the temporal relationships between longitudinal flexural normal faults and thrusts and related folds when the thrust propagation sequence is a) forward-breaking or "piggy-back" and b) break-back. The upper drawings in a) and b) are the oldest stages, while the lower drawings in a) and b) are the younger ones. Structures numbered as 1 are the oldest ones, whereas those numbered as 2 are the youngest ones. The dips of the layers and faults, as well as the angles between them, do not represent actual values, but have been used to better visualize the figure.

orogen in the northwest portion of the Iberian-Peninsula (e.g., Julivert, 1971, 1979, 1981, 1983; Savage, 1979, 1981; Pérez-Estaún et al., 1988; Pérez-Estaún and Bastida, 1990; Alonso et al., 1992; Aller et al., 2004). Normal faults, whose cross-cutting relationships indicate that predate thrusts and folds and were developed in undeformed rocks, have been documented in some localities (e.g., Masini et al., 2010a, 2010b; Bulnes et al., 2016, 2019; Uzkeda et al., 2022). A cursory analysis might lead us to define two unrelated deformation events: an older extensional one and a younger contractional one. However, as mentioned above, in fold-and-thrust belts there are other possible scenarios where these structures may result from the same deformational event (e.g., Poblet and Lisle, 2011). The main features of these normal faults suggest that they could be interpreted as flexural normal faults related to foredeep flexures later on folded and thrusted as the contractional deformation propagated towards the foreland. The case presented here is not the first one of its kind. Thus, in the Apennines, where normal faults deformed by thrusts occur (e.g., Scisciani, 2009; Masini et al., 2011; Calamita et al., 2018), some normal faults have been interpreted as related to the orogenic process, resulting from lithospheric bending of the foredeep (e.g., Scisciani et al., 2001, 2002).

The application of the methodologies described in this article to the field example intends to address the following specific goals.

i) Decipher the main features of these Cantabrian Zone normal faults through a detailed structural analysis and prove that they are flexural normal faults.
ii) Figure out the orientation of the orogenic front in the past and its angle with the tectonic transport direction through the study of the Cantabrian normal faults and their comparison with published tectonic transport vectors. Verify whether the orogenic front aligns with the curved structural pattern of the Ibero-Armorican or Asturian Arc.
iii) Investigate whether these Cantabrian normal faults can be key elements for determining the type of thrust propagation sequence by inferring it and contrasting it with data published in the literature.
iv) Provide information about the main characteristics of the old flexure in the western part of the Cantabrian Zone through the study of normal faults.
v) Unravel the meaning of some normal faults perpendicular with respect to the most common set of Cantabrian normal faults through the analysis of these normal faults and published geological maps.

The Cantabrian Zone is an excellent natural laboratory to address this study (Fig. 3). Thus, abundant literature information is available about the Cantabrian Zone structure and cartographic pattern (see references above) to cross-check the results derived from the analysis of normal faults. In addition, the quality of some outcrops is exceptional; thus, a simple observation is sufficient to describe the characteristics of the normal faults, thrusts and folds and their temporal relationships. Finally, this is the first time that the normal faults preceding the thrusts

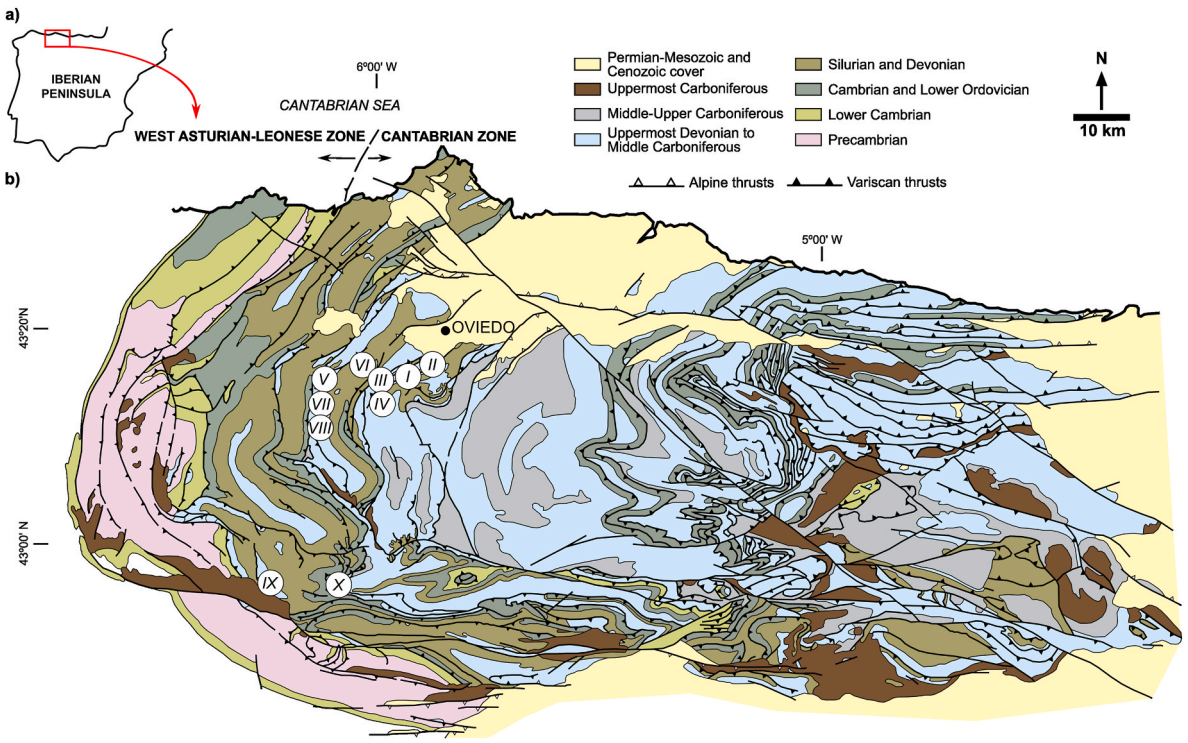

Fig. 3. a) Iberian Peninsula map showing the location of the map depicted in b). b) Geological map of the Cantabrian Zone, located at the core of the Ibero-Armorican or Asturian Arc (modified from Alonso et al., 2009b). The small circles including a number in the western part of the Cantabrian Zone show the location of the studied outcrops. I: La Mortera, II: Tellego, III: Tenebredo, IV: Dosango, V: Baselgas, VI: Castañedo del Monte, VII: Linares, VIII: Bandujo, IX: Vega de los Viejos and X: San Emiliano.

and related folds are described in detail and interpreted as flexural normal faults in the Cantabrian range.

2. Part I: flexural normal faults, foredeep flexures and fold-and-thrust belts

2.1. Longitudinal flexural normal faults

2.1.1. Development of longitudinal flexural normal faults in the foredeep flexures of fold-and-thrust belts

In front of a fold-and-thrust belt, during its emplacement, a foreland basin develops. An ideal foreland basin system is composed of four depozones: wedge-top, foredeep, forebulge, and back-bulge, generated as a result of the flexural response to the fold-and-thrust belt load (e.g., Beaumont, 1981; Flemings and Jordan, 1989; DeCelles and Giles, 1996; DeCelles, 2011). From a geometrical point of view, the foredeep is a large, deep trench next to the orogenic front, whose opposite boundary dips in the same direction as the basal detachment of the fold-and-thrust belt. The forebulge is a small, convex low rise and the back-bulge is a broad region with a shallow concave geometry. The forebulge is the result of a flexural uplift. In contrast, both the foredeep and the back-bulge result from flexural subsidence, with the foredeep being the region that experienced high subsidence compared to the mild subsidence experienced by the back-bulge.

Here, we will focus on the kinematic evolution of the foreland-basin main flexure. To do so, we will simplify its geometry to an approximately monoclinal anticline resulting from a bending mechanism (e.g., Bradley and Kidd, 1991; Doglioni, 1995) (Fig. 1). The main structural elements of this monoclinal fold are an inclined limb (foredeep), a subhorizontal limb (back-bulge and regions farther from the undeformed orogenic front), and a hinge zone (forebulge) located between both limbs. A steep axial surface and an approximately horizontal fold axis, both subparallel to the fold-and-thrust belt front, run through the hinge zone (Fig. 1). Flexures in front of fold-and-thrust belts have been recognized both in the subsurface using seismic data (e.g., Bradley and Kidd, 1991; Chou and Yu, 2002) and at the surface in geological maps (e.g., Dreyfuss et al., 1968).

In a simple picture where a fold-and-thrust belt advances toward the foreland, the foredeep flexure is subjected to two different amplification mechanisms. Firstly, as the fold-and-thrust belt advances, the subhorizontal limb layers roll through the flexure axial surface (e.g., Bradley and Kidd, 1991; Doglioni, 1995), which is an active axial surface, and become incorporated into the flexure inclined limb through a mechanism known as hinge migration (e.g., Suppe, 1983; Suppe and Medwedeff, 1990) (Fig. 4). Secondly, as the fold-and-thrust belt grows, the load over the foredeep increases causing subsidence (e.g., Doglioni, 1993; DeCelles and Giles, 1996), which leads to a progressive increase in the dip of the flexure inclined limb and a consequent decrease in the flexure interlimb angle through a mechanism known as limb rotation (e.g., Hardy and Poblet, 1994; Epard and Groshong Jr, 1995) (Fig. 4). Thus, at least during the initial stages of evolution, while the fold-and-thrust belt advances and growths before reaching the critical taper angle, the flexure might result from a mixture of hinge migration and limb rotation. The combination of these two mechanisms in variable proportions (e.g., Poblet and McClay, 1996; Poblet et al., 1997) has been proved to occur in nature and be responsible, for instance, for the amplification of both subsurface (e.g., Soleimany et al., 2011; Valero et al., 2015) and surface (e.g., Poblet et al., 1998; Alonso et al., 2011) folds. Nevertheless, the fold-and-thrust belt dynamics may change at some point according to the critical taper theory, and this may influence the flexure amplification mechanisms that operate and/or their proportions.

Maps (e.g., Poblet, 2020) and sections (e.g., Salvini and Storti, 2004) across theoretical models of folds formed by combination of hinge migration and limb rotation show that rocks undergo deformation when they roll through an active axial surface that separates a subhorizontal limb from an inclined limb of a monocline. Rock and clay laboratory

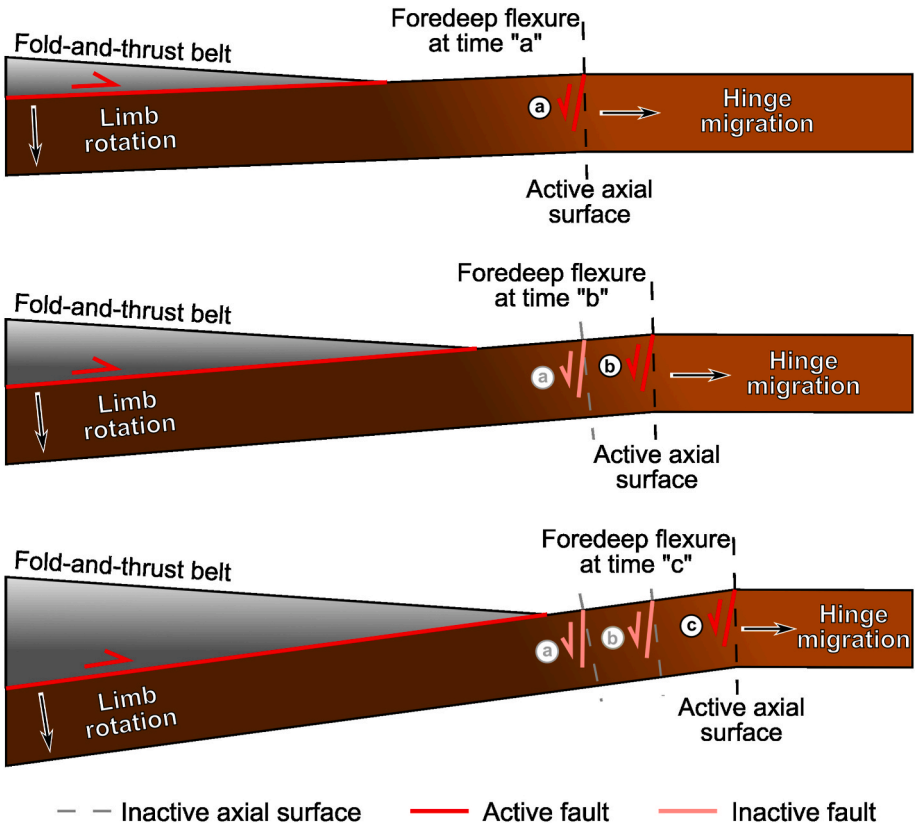

Fig. 4. Idealized schematic cross-sections showing the development of a foredeep flexure and associated longitudinal flexural normal faults by combination of hinge migration and limb rotation (modified from Rodríguez et al., 2022c). The upper section is the oldest stage and the lower section is the youngest one. The dips of the layers, faults and axial surfaces, as well as the angles between them, do not represent actual values, but have been used to better visualize the figure.

experiments of both contractional (e.g., Chester et al., 1991) and extensional (e.g., Cloos, 1968; Xiao and Suppe, 1992) folds show that this deformation is usually accommodated through fracturing. In both theoretical models and physical experiments, these fractured rocks become part of the monocline inclined limb as the active axial surface migrates relative to the rocks (Fig. 4). Thus, although the foredeep flexure is a ductile structure, the combination of these amplification mechanisms, i.e., hinge-migration and limb-rotation, would explain the presence of brittle structures, i.e., fractures, in the foredeep-flexure hinge zone, as well as along the entire foredeep-flexure inclined limb. Regarding the distribution and type of deformation in the folded layers, one of the most commonly cited reasons to explain why normal faults occur in relation to the foredeep flexure is that a certain component of tangential longitudinal strain may take place (e.g., Bradley and Kidd, 1991; Doglioni, 1995). Thus, brittle structures, such as normal faults (Fig. 1), would develop in the external arc of the flexure above the neutral surface, according to the tangential longitudinal strain theory developed by Ramsay (1967) and Ramsay and Huber (1987).

Regarding the relative age of the flexural normal faults, the closer they are to the orogenic belt front, the older they are (e.g., Rodríguez et al., 2022c). As the fold-and-thrust belt advances towards the foreland, the active axial surface that separates the flexure inclined limb from the subhorizontal limb also migrates towards the foreland incorporating new rocks into the inclined limb at the expense of subhorizontal limb rocks, while developing new normal faults along its path (Fig. 4). Thus, the orogenic front approaches the normal faults developed in the older stages in such a way that it may even override them.

The strike of normal faults related to folds caused by bending is typically parallel to the minimum curvature direction according to the Gaussian curvature theory (e.g., Lisle, 1994; Masaferro et al., 2003; Fiore Allwardt et al., 2007). The foredeep flexure is a fold caused by bending. Since the minimum curvature direction of the foredeep flexure is its axis, the strike of the flexural normal faults is supposed to be parallel to the flexure axis. The fronts of fold-and-thrust belts, and their related foredeep flexures may be linear but often display open arcuate shapes in map view (e.g., Elliott, 1976) (Fig. 5). In these cases, the flexure may be wider in the most advanced part of the front and narrow progressively as it approaches the front tips util it disappears. Therefore, the foredeep flexure axis and the associated flexural normal faults may not be strictly parallel to the orogenic front but are approximately so. Tectonic transport vectors are usually perpendicular or form a high angle with the fronts of fold-and-thrust belts (Fig. 5). Thus, the most advanced part of the orogenic front is perpendicular to the tectonic transport vector, but as we move toward the lateral thrust tips, where the front has advanced less, the front is oblique to the tectonic transport vector. Therefore, flexural normal faults are perpendicular to the tectonic transport vector in the most advanced part of the front, but oblique to it at the lateral terminations. The more open the original arcuate shape of the belt front, the more perpendicular the tectonic transport vector to the flexural normal faults everywhere, and vice versa.

As mentioned above, the subsidence, which is dependent on the weight of the fold-and-thrust belt, influences the dip of the inclined limb and interlimb angle of the foredeep flexure, and therefore, its hinge zone curvature. According to the Gaussian curvature theory, the fracturing intensity correlates to the curvature, such that greater curvature induces greater fracturing intensity (e.g., Lisle, 1994; Masaferro et al., 2003; de Oliveira Neto et al., 2025). However, some studies have shown that, aside from curvature, lithology is a determining factor (Watkins et al., 2020) and that other local deformation mechanisms may exist (Fiore Allwardt et al., 2007). Nevertheless, in the context studied here, it is very likely that the lithology remains constant and that, although other local deformation mechanisms may be present, the main one is

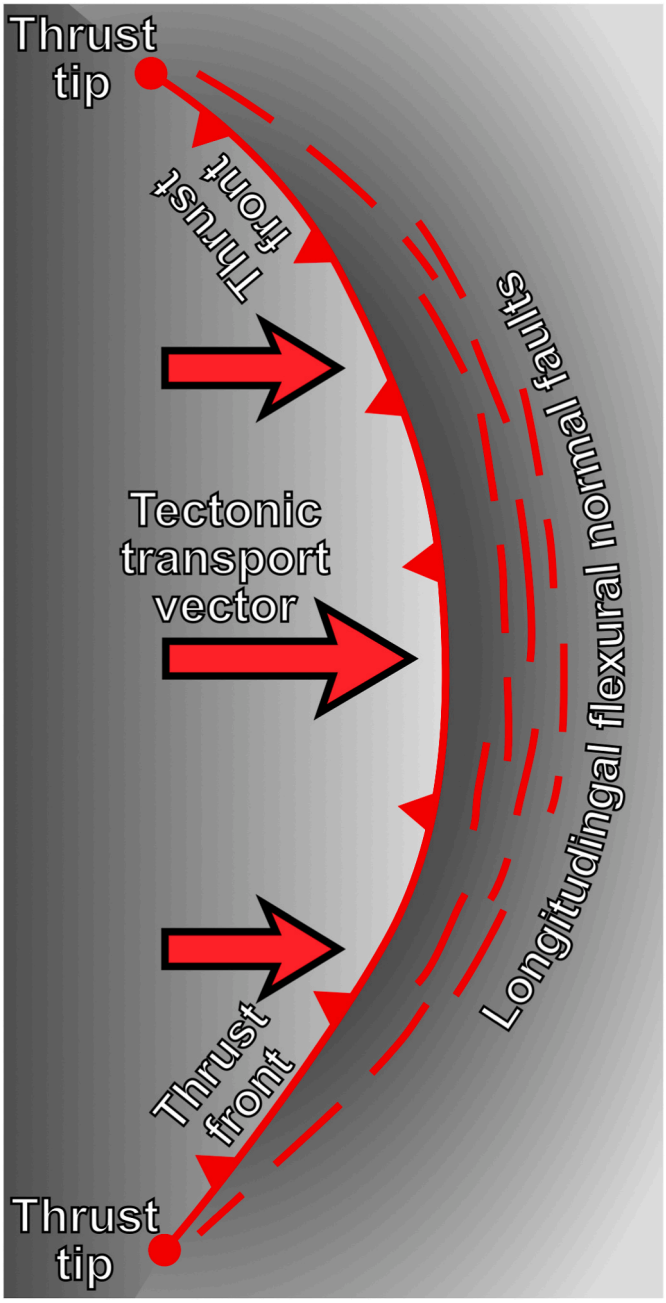

Fig. 5. Idealized schematic map showing an arcuate thrust belt front and the longitudinal flexural normal faults developed in the foredeep flexure.

curvature. Thus, the weight of the fold-and-thrust belt may exert a strong influence on the fracturing intensity related to the flexural normal faults. The greatest fracturing intensity is expected in the portion of the foredeep flexure located in front of the most advanced part of the orogenic front, where the belt is supposed to be heavier, gradually decreasing towards its lateral terminations (Fig. 5).

As stated above, the foredeep flexure and associated flexural normal faults develop in the footwall of the frontal thrust of a fold-and-thrust belt. In a forward-breaking or "piggy-back" thrust-propagation sequence, which is the most common in nature (e.g., Butler, 1987), thrust sheets are progressively younger towards the foreland, i.e., thrust sheets develop in the footwall of older thrust sheets (e.g., Butler, 1987; McClay, 1992). Thus, when a new frontal thrust sheet forms, the new folds and thrusts overprint the flexural normal faults developed in the previous stage. In addition, a new foredeep flexure and associated flexural normal faults develop in the footwall of the new frontal thrust of the fold-and-thrust belt. As a result, the different thrust sheets include flexural normal faults deformed by contractional structures (Fig. 2a). In contrast, in a break-back thrust propagation sequence, thrust sheets become progressively younger towards the hinterland, i.e., thrust sheets develop in the hangingwall of older thrust sheets (e.g., Butler, 1987; McClay, 1992). Thus, when a new thrust sheet forms in the frontal part of a fold-and-thrust belt, it does not interfere with the flexural normal faults, and therefore, they are not deformed. In this case, if normal faults would develop only in the footwall of the frontal thrust, then they would be undeformed and the different thrust sheets would not include normal faults within them. In case gentle flexures and associated normal faults related to the emplacement of each thrust sheet were to develop, then there would be flexural normal faults within each thrust sheet and they would postdate the contractional structures (Fig. 2b).

2.1.2. *Recognizing longitudinal flexural normal faults*

In a typical forward-breaking thrust sequence, the flexure and flexural normal faults generated in the final stages of fold-and-thrust belt evolution are found in the foredeep, while the flexure and flexural normal faults linked to initial and intermediate stages of fold-and-thrust belt development should be found in different thrust sheets within the fold-and-thrust belt (Fig. 2a). Both foredeep flexures and related flexural normal faults developed in final stages of fold-and-thrust belt evolution are easy to recognize in relatively undeformed foreland basins located in front of fold-and-thrust belts because both are still preserved (e.g., Bradley and Kidd, 1991; Chou and Yu, 2002; Rodríguez et al., 2021). Identifying foredeep flexures and related flexural normal faults linked to initial and intermediate stages of fold-and-thrust belt development is much more difficult. The foredeep flexures are usually much gentler structures than the thrusts and folds, and therefore, the contractional deformation may obliterate them as thrust systems and fold trains propagate. However, recognizing flexural normal faults developed during initial and intermediate stages of fold-and-thrust belt development is still possible. Although these flexural normal faults may have been modified due to the superposition of thrusts and related folds as the fold-and-thrust belt advanced towards the foreland (e.g., Scisciani et al., 2001, 2002), a detailed structural analysis usually allows their identification (e.g., Calamita et al., 2018) unless the contractional deformation caused by the development of the fold-and-thrust belt is extremely intense and complex. The following criteria may help to identify them.

One of the main aspects to investigate in order to recognize these ancient flexural normal faults is the temporal relationship between them and the contractional structures. As mentioned, it is very likely that the flexural normal faults predate the thrust faults and related folds developed in the same thrust sheet (Table 1). Thus, the following types of crosscutting relationships between structures are expected: normal faults partially or totally reactivated as reverse faults, normal faults cut and offset by thrusts or by bedding surfaces that have undergone flexural slip consistent with folds, normal faults tilted on fold limbs, folded normal faults, and normal faults showing buttressing-related structures in both their hangingwalls and footwalls. However, if they are indeed flexural normal faults, they should be coeval with the thrusts and folds developed in the overlying thrust sheet (Table 1). To verify this temporal relationship, cross-cutting relationships cannot be used, as these structures do not interact with each other. Therefore, it is advisable to use either absolute dating methods, such as radiometric dating of fault slickensides developed in normal fault and thrust surfaces, or dated growth strata, if syn-extensional beds associated with flexural normal faults and syn-contractional beds associated with thrusts and related folds in the overlying thrust sheet occur.

Aside from the relative age between normal faults and contractional structures, another feature that allows distinguishing flexural faults from other faults is that they may show normal but also reverse offset in their current attitude (Table 1). However, when bedding is unfolded and restored to a horizontal position, and the normal faults are rotated

Table 1
Diagnostic criteria to identify longitudinal flexural normal faults formed during initial and intermediate stages of fold-and-thrust belt development.

		DIAGNOSTIC CRITERIA
TIMING OF THE NORMAL FAULTS	*WITH RESPECT TO FOLDS AND THRUSTS IN THE SAME THRUST SHEET*	Predate
	WITH RESPECT TO FOLDS AND THRUSTS IN THE OVERLYING THRUST SHEET	Coeval
NORMAL FAULT KINEMATICS	*PRESENT-DAY*	Normal or reverse
	ORIGINAL	Normal
ANGULAR RELATIONSHIPS BETWEEN BEDDING AND CONJUGATE NORMAL FAULTS		Bisects obtuse angle
SLIP, FREQUENCY AND LENGTH OF THE NORMAL FAULTS WITH RESPECT TO FOLDS AND THRUSTS		Smaller
AGE OF THE ROCKS AFFECTED BY THE NORMAL FAULTS		Youngest ones
ANGLE BETWEEN THE STRIKE OF THE NORMAL FAULTS AND THE CONTRACTIONAL TECTONIC TRANSPORT VECTOR		Perpendicular or high angle

accordingly, the flexural normal faults always exhibit normal offset (Table 1). If conjugate flexural normal faults occur, the stratification should bisect the obtuse angle between the faults, as they developed when the stratification was either horizontal or had a very low dip (Table 1). The flexural normal faults result from relatively low extension values and that explains why they usually exhibit relatively low slips (e.g., Chou and Yu, 2002) smaller than those of the thrusts, and are usually less abundant and/or shorter than the thrusts and related folds (Table 1). They are usually developed in the syn-contractional beds and youngest layers of the pre-contractional stratigraphic succession, as they developed in the outer arc of the foreland flexure due to tangential-longitudinal strain (Table 1). The tectonic transport vector of the overlying thrust sheet where the normal faults are developed, may also be used as a diagnostic element to identify flexural normal faults. The direction of the tectonic transport vector is available in many orogens, obtained through analysis of cutoff line maps, kinematic indicators collected on thrust surfaces, in rocks adjacent to them, in fault rocks, etc. Once the normal faults are rotated to their original attitude, if they are indeed flexural normal faults, in approximately linear fold-and-thrust belts their strike should either be perpendicular to or form a high angle with the tectonic transport vector of the overlying thrust sheet (Fig. 5 and Table 1).

2.1.3. *Longitudinal flexural normal faults as indicators of orogenic front orientation, age and thrust propagation sequence of fold-and-thrust belts, as well as curvature and interlimb angle of foredeep flexures*

Flexural normal faults can provide interesting information about the features of the fold-and-thrust belt and the foredeep flexure as we show below. Usually, the study of structures developed within a thrust sheet supplies information about the past and present structure of the thrust sheet itself, however, the study of old flexural normal faults provides information about the past structure of the thrust sheet itself when it was a foredeep, but also about the overlying thrust sheet when it was the frontal one of the fold-and-thrust belt. Below, we briefly describe some of the potential results that can be obtained from the analysis of flexural normal faults and the procedures to achieve them.

i) Age of the fold-and-thrust belt. When the flexural normal faults exhibit dated growth strata, i.e., syn-extensional beds, or their slickensides have been dated, it becomes possible to estimate the age of the normal faults and, therefore, the age of the causative foredeep flexure, as well as the emplacement age of the fold-and-thrust belt (Rodríguez, 2020; Rodríguez et al., 2021, 2022a), since all these elements developed simultaneously (Fig. 6).

iI) Orientation of the fold-and-thrust belt front. The strike of flexural normal faults supplies the approximate orientation of the orogenic front (Figs. 1, 5 and 6). When the direction of the tectonic transport vector of the fold-and-thrust belt is available, the angle between the strike of the flexural normal faults and the tectonic transport vector may indicate which part of the orogenic front we are dealing with. The angle should be 90° in the central part of the belt, whereas it should be smaller when approaching the belt front tips or lateral parts of salients and recesses.

iii) Thrust propagation sequence. The temporal relationships between flexural normal faults and thrusts and folds provide information about the type of thrust propagation sequence (Figs. 2 and 6). Thus, flexural normal faults older, and consequently deformed, by the thrusts and folds present in different thrust sheets suggests that the thrust propagation sequence was forward-breaking or "piggy-back". On the contrary, the absence or the presence of undeformed normal faults in the different thrust sheets could be indicative of a break-back type thrust propagation sequence.

iv) Geometry of the foredeep flexure and tectonic load. Measurements of the fracturing intensity using flexural normal faults may reflect in a qualitative way the flexure curvature degree, the dip of the flexure inclined limb, the flexure interlimb angle, and perhaps the tectonic load caused by the fold-and-thrust belt (Fig. 6). Since we are dealing with an anticlinal monocline whose inclined limb dip increases as the belt load increases, a greater fracture intensity indicates a greater curvature, a steeper flexure inclined limb, a lower flexure interlimb angle, and perhaps a higher tectonic load as well. For fracturing intensity measurements to be comparable, they should be carried out in rheologically equivalent rocks, as more competent lithologies tend to accommodate deformation in a more brittle manner than less competent lithologies.

v) Rates of fold-and-thrust belt advance. If dated flexural normal faults are found at progressively more distant locations from the fold-and-thrust belt front responsible for the flexure, and their associated syn-extensional strata or ages indicate that the more distant faults are younger, across-strike flexure propagation rates may be quantified and, consequently, fold-and-thrust belt advance rates. This can be achieved by measuring the distance between the normal faults perpendicular to their strike and dividing it by the time elapsed between the development of each fault (Rodríguez, 2020; Rodríguez et al., 2021, 2022a).

vi) Variations in the fold-and-thrust belt front and in the foredeep flexure over time. Additionally, measuring the strike of these normal faults progressively farther from the belt front described above could reveal the approximate orientation of the belt front over time, and verify whether it remained constant or varied during its emplacement. Similarly, measuring fracturing intensity due to normal faults progressively farther from the fold-and-thrust belt front would allow us to determine temporal variations in the flexure curvature degree, the dip of its inclined limb and its interlimb angle, and perhaps in the belt tectonic load, and whether these values remained constant or varied during the belt advance (Fig. 6).

vii) Rates of along-strike deformation migration. If dated flexural normal faults are mapped at different locations, all at approximately the same distance from the fold-and-thrust belt front, and the faults are younger towards one particular direction, it is

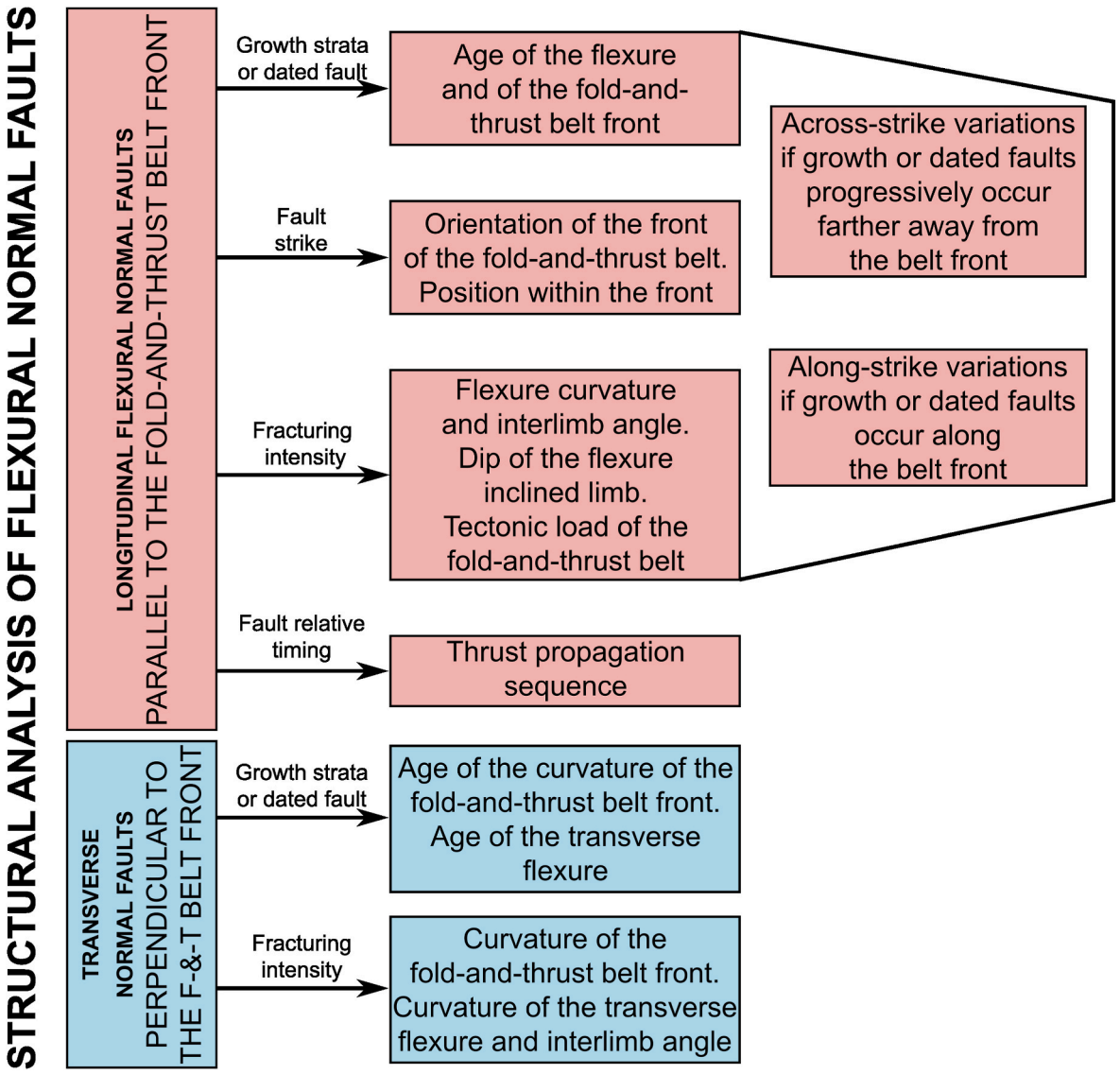

Fig. 6. Flow chart showing the type of information that may be obtained regarding fold-and-thrust belts and foredeep flexures from the structural analysis of longitudinal flexural normal faults and transverse normal faults.

possible to quantify approximate along-strike flexure propagation rates and, therefore, along-strike deformation migration caused by the belt advance. This can be done by measuring the distance between normal faults parallel to the strike of the faults and dividing it by the time elapsed between the development of each fault.

viii) Along-strike variations in the fold-and-thrust belt front and in the foredeep flexure. Moreover, measuring the strike of the normal faults at different locations, all at approximately the same distance from the orogenic front, may help to determine whether the belt front orientation along strike was constant or it had an arched geometry (Fig. 5). Similarly, determining fracturing intensity due to flexural normal faults at different locations, all at approximately the same distance from the orogenic front, would reveal whether the flexure curvature degree, the dip of its inclined limb and its interlimb angle, and perhaps the belt tectonic load, remained constant along strike or varied throughout the belt (Fig. 6).

2.2. Transverse normal faults

2.2.1. Development of transverse normal faults in the foredeeps of fold-and-thrust belts

The strike of most flexural normal faults related to a foredeep flexure caused by a fold-and-thrust belt is parallel to the flexure axis and almost parallel to the fold-and-thrust belt front. However, normal faults approximately perpendicular to the fold-and-thrust belt may develop, fundamentally due to two distinct causes: the original arched shape of the fold-and-thrust belt front (Fig. 5) and along-strike variations in the tectonic load within the fold-and-thrust belt.

The development of an arched fold and thrust belt involves horizontal stretching parallel to the arc trend. Thus, the length of any pre-arching linear marker increases as the fold-and-thrust belt advances towards the foreland. This extension is accommodated through transverse normal faults, i.e., perpendicular to the arc, whose strike varies progressively along the arc depending on the orogenic front strike (Doglioni, 1995).

Along-strike variations in the load of the fold-and-thrust belt, responsible for transverse flexures and associated flexural normal faults, may result from diverse causes. Among these, the following stand out:

along-strike terminations of thrust sheets, development of tear faults during thrust emplacement, lateral and/or oblique ramps, and occurrence of salients and recesses (Fig. 7). The reasons that can cause these types of structures are diverse: changes in the rheological properties of the pre-orogenic succession along strike, variations in the syn-contractional sedimentation rate along strike, along-strike variations in the magnitude of the tectonic transport vector, and pre-existing basement structures that hinder the advancement of portions of a thrust sheet.

2.2.2. *Recognizing transverse normal faults. Indicators of age and curvature of the orogenic front and transverse flexures*

Transverse normal faults are located in specific areas. Thus, transverse normal faults caused by arc curvature (Doglioni, 1995) are expected to be found in regions where there are significant variations in the strike of the orogenic front, or in other words, in the strike of the longitudinal faults. Transverse normal faults caused by lateral/oblique structures are expected to be located in regions near lateral/oblique structures of certain dimensions developed in the overlying thrust sheet. Transverse normal faults typically coexist with longitudinal normal faults, since the longitudinal ones are developed along the entire front of the fold-and-thrust belt. Therefore, if we find only one set of faults, it is most likely longitudinal normal faults. Regarding the timing, transverse normal faults are coeval with longitudinal flexural normal faults, since both sets of normal faults are related to simultaneous phenomena: arched belt geometry or lateral/oblique structures in the case of transverse faults, and fold-and thrust belt advance towards the foreland in the case of longitudinal faults. As with longitudinal normal faults, in a typical forward-breaking thrust sequence, transverse normal faults predate the folds and thrusts developed within the same thrust sheet, but are synchronous with the folds and thrusts developed in the overlying thrust sheet. Also, similar to longitudinal normal faults, bedding should bisect the obtuse angle between conjugate transverse normal faults, and transverse normal faults should exhibit small displacements, and be smaller and less abundant than the folds and thrusts. Unlike longitudinal normal faults, the strike of transverse normal faults should be approximately parallel to, or form a low angle with the tectonic transport vector of the overlying thrust sheet.

In general, flexures caused by lateral or oblique structures are supposed to be more open than flexures parallel to the front of the fold-and-thrust belts, since lateral and oblique structures are also smaller in size. Therefore, flexural normal faults related to transverse flexures are expected to exhibit lower slips, dimensions and/or frequency than flexural normal faults related to longitudinal flexures parallel to the fold-and-thrust belt front. Lateral structures are parallel to the tectonic transport vector and result in a sharp change in the tectonic load caused by the fold-and-thrust belt. Thus, on one side of the lateral structure the load is greater, while on the other side it is smaller. This phenomenon likely leads to narrow transverse flexures with well-defined boundaries, and therefore, transverse flexural normal faults concentrated in narrow bands. However, oblique structures, by maintaining an oblique relationship with the tectonic transport vector, cause a progressive gradient in the tectonic load induced by the fold-and-thrust belt during its advance. In this case, there may not be a defined boundary separating a higher tectonic load zone from a lower tectonic load zone. Thus, the flexures resulting from oblique structures may be wider and their boundaries diffuse, and therefore, their associated transverse flexural normal faults may be widespread along a broader area.

Similar to longitudinal normal faults, dated transverse normal faults can provide information on the timing of the orogenic front curvature or of the lateral/oblique structures responsible for their formation (Fig. 6). Measurements of their fracturing intensity may supply information on the curvature degree of the orogenic front or on the curvature of the transverse flexure and its interlimb angle.

3. Part II: western portion of the Cantabrian Zone

3.1. *Geological setting*

The Cantabrian Zone, located in the north-northwest portion of the Iberian Peninsula, is a foreland fold-and-thrust belt developed mainly during Carboniferous (e.g., Lotze, 1945; Julivert et al., 1972) (Fig. 3). It belongs to the Variscan orogen which, at least, extends from Central Europe to Iberia. The Cantabrian Zone involves a Palaeozoic succession

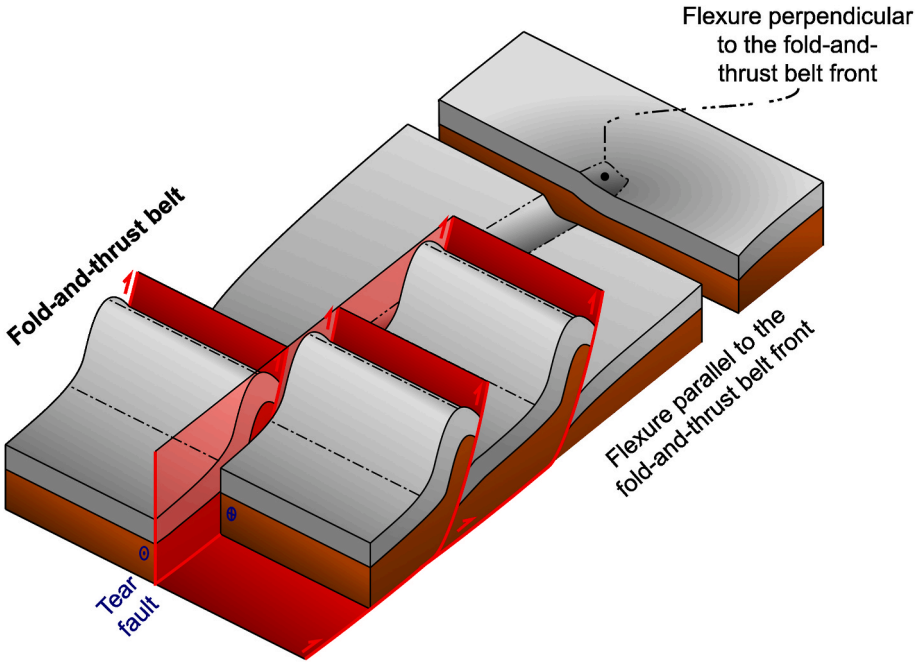

Fig. 7. Idealized schematic block diagram showing the development of a flexure perpendicular to the tectonic transport direction caused by a tear fault in the fold-and-thrust belt. The dashed-dotted lines are axial traces of the folds. The dips of the layers and faults, as well as the angles between them, do not represent actual values, but have been used to better visualize the figure.

from Cambrian to Carboniferous made up of alternations of different types of carbonate and detrital rocks, as well as some scarce volcanic rocks. In map view, it shows an arcuate shape with the inner core to the east. This belt is located in the core of the Ibero-Armorican or Asturian Arc (e.g., Suess, 1892; Lotze, 1945), so that the main structures strike E-W in the north branch of the arc and progressively bend to NE-SW, to NW-SE and to E-W in the south branch (Fig. 3). In cross-sectional view, this belt has a wedge morphology tapering towards the east, i.e., towards the foreland, bounded by a W-dipping basal detachment. The structure of the Cantabrian Zone is typically thin-skinned and is made up of imbricate thrust systems, although antiformal stacks and duplex also occur, and different types of fault-related folds, such as fault-bend folds, fault-propagation folds and detachment folds (e.g., Julivert, 1971, 1983; Savage, 1979, 1981; Pérez-Estaún et al., 1988; Pérez-Estaún and Bastida, 1990; Alonso et al., 1992; Aller et al., 2004). Strain in the Cantabrian Zone is not very intense, and cleavage is only present in some areas. This region developed under diagenetic conditions, and only a few localities underwent low to very low-grade metamorphism.

Several extensional events including normal faulting, reactivation of some previous faults, heating, and/or uplift led to the opening of the Bay of Biscay located to the north of the Iberian Peninsula. They occurred in Permian times (Julivert et al., 1971; Suárez-Rodríguez, 1988; Lepvrier and Martínez-García, 1990; López-Gómez et al., 2019), from Middle Jurassic to the lower part of the Late Jurassic (Fernández-López and Suárez Vega, 1981; Valenzuela et al., 1986, 1989; Lepvrier and Martínez-García, 1990; Uzkeda, 2013; Uzkeda et al., 2013, 2016, 2018, 2025; Magán, 2024) and from the upper part of the Late Jurassic to the lower part of the Early Cretaceous (Alonso et al., 2016; Cadenas and Fernández-Viejo, 2017; Magán, 2024; Uzkeda et al., 2025).

From the Eocene until the beginning of the Oligocene (Magán, 2024), selective reactivation of previous structures, and generation of new thrusts and uplifts occurred (e.g., Lepvrier and Martínez-García, 1990; Alonso et al., 1996, 2009, 2016; Pulgar et al., 1999; Uzkeda, 2013; Uzkeda et al., 2013, 2016, 2018, 2025; Magán et al., 2022; Magán, 2024), as a consequence of an Alpine contractional event induced by the convergence between the Iberian and Eurasian tectonic plates. This event led to the formation of the Cantabrian Mountains in the north part of the Iberian Peninsula which involve the Cantabrian Zone.

During Early Pleistocene or even before (e.g., Álvarez-Marrón et al., 2008), the marine abrasion platform in the north coast of the Iberian Peninsula, underlain by Cantabrian-Zone Palaeozoic rocks, was uplifted above present-day sea level, giving rise to “rasas” (e.g., Flor, 1983; Mary, 1983). Additional neotectonic activity occurred, such as reactivation of previous faults (e.g., Gutiérrez Claverol et al., 2006; Álvarez-Marrón et al., 2008) and small magnitude earthquakes (e.g., López-Fernández et al., 2004).

3.2. Methodology

Several field campaigns in the western part of the Cantabrian Zone have allowed us to collect data regarding a set of normal faults developed prior to the folds and thrusts when the layers were undeformed (e.g., Masini et al., 2010a, 2010b; Bulnes et al., 2016, 2019; Uzkeda et al., 2022). Firstly, precise orientation measurements of bedding, normal faults, as well as contractional structures such as folds and thrusts, have been taken at various localities, aiming for them to be representative of some thrust sheets defined in the western part of the Cantabrian Zone. Care has been taken to avoid confusing the ancient normal faults studied here with younger structures, paying close attention to cross-cutting relationships between extensional and contractional structures. Despite visiting many locations, observations have been successfully made at fourteen outcrops. Some of these outcrops have been treated jointly due to their proximity and the similarity of the collected data.

Subsequently, in the laboratory, the studied outcrops have been placed in their correct geographic positions on a Cantabrian-Zone geological map. The two rules employed to decipher which thrust sheet was located at the front of the fold-and-thrust belt at the time of formation of the flexural normal faults are briefly described below.

i) The general tectonic transport sense in the western part of the Cantabrian Zone is broadly from westward to eastward (e.g., Julivert et al., 1968; van den Bosch, 1969; De Sitter and Van den Bosch, 1969; Heredia, 1984; Alonso et al., 1989; Gutiérrez Alonso, 1992; Bulnes and Marcos, 2001, Caldera Grau, 2016; De Paz Álvarez, 2023), so that the thrust sheet responsible for the formation of the normal faults would always be located westwards of them.
ii) The thrust sheet located at the fold-and-thrust belt front when the normal faults developed should overthrust the thrust sheet where the normal faults have been mapped.

The collected data in each outcrop have been plotted on an equal-area projection, using the software Stereonet (Allmendinger et al., 2013). Next, also using the same software, the bedding of the rocks affected by normal faults has been rotated back to horizontal, and the normal faults have been rotated accordingly to determine their original orientation at the time of their formation. This procedure has been carried out in two different ways. In those outcrops where the normal faults were developed on a fold limb, the fold axis—obtained from an equal-area plot of folded bedding measurements—has been used to carry out the rotations. If the fold axis had a certain plunge, a double rotation has been performed. First, the fold axis has been rotated to a horizontal position along with the layers and faults, and then the layers have been unfolded using the horizontal axis obtained in the previous step. However, in those outcrops where the normal faults were developed in rocks located within a thrust sheet bounded by inclined thrusts, so that the orientation of the fold responsible for the layer dip was unclear, the stratification strike has been used to rotate the layers to horizontal.

The equal-area plots including rotated bedding and normal faults have been examined to determine how many families of faults could be detected. The strike of the rotated normal faults has been compared with the orientation of the tectonic transport vectors of the thrust sheets related to the studied outcrops. The information about the tectonic transport vectors has been obtained from the literature. The normal faults approximately perpendicular or at high angle to the tectonic transport vectors have been interpreted to be longitudinal flexural normal faults parallel to the fold-and-thrust belt front at the time of formation of the normal faults, and the angle between their strike and the tectonic transport vector has been measured. The normal faults approximately parallel or at a low angle to the tectonic transport vectors have been assumed to be transverse normal faults.

The fracturing areal intensity due to normal faults parallel to the orogenic front has been estimated in some studied outcrops, using the sampling method known as circular windows (Mauldon et al., 2001; Rohrbaugh et al., 2002). The fracturing areal intensity, defined as the fracture length per unit area, has been calculated using a mathematical relationship between the number of fractures intersecting the circular window and its radius as proposed by the authors who designed the circular windows method. This has allowed us to obtain qualitative information about the degree of flexure curvature, the dip of the flexure inclined limb, and the flexure interlimb angle.

In order to assess whether the fracturing intensity measurements carried out in different lithologies were comparable, Schmidt-hammer rebound values have been measured. The Schmidt hammer rebound values have been collected using an N-type Schmidt hammer manufactured by the company Proceq, with a normalized impact energy of 2.207 Nm and with a correction factor of 0.96. According to the Proceq (2016) manual instructions, this device does not need corrections related to the gravity force. The collected data have been treated using the Standard Test Method for Determination of Rock Hardness by Rebound Hammer Method ASTM D 5873 (American Society for Testing and Materials, 2001; usually know as ASTM). This method requires 10 impacts in each

location and a mean is calculated; individual rebound values that diverge more than 7 from the calculated mean are discarded and a new mean is calculated using the remaining values. In order to avoid wrong measurements, the rules recommended in Aydin and Basu (2005), Proceq (2016) and Poblet et al. (2022) to collect the data have been followed, i.e., impacts as perpendicular as possible to the rock faces to be measured and in close but different places, avoiding rough surfaces and rock faces with alteration patina and/or moss/lichens, and under similar moisture conditions.

Concerning the determination of the thrust propagation sequence, detailed fieldwork has been conducted in all the analysed outcrops to establish the relative age of the normal faults and contractional structures—folds and thrusts—, based on the analysis of cross-cutting relationships between them.

In those outcrops where families of normal faults parallel or slightly oblique to the tectonic transport vectors, i.e., transverse normal faults, have been identified, efforts have been made to check whether there was a significant change in the orientation of the orogenic front in that region, as inferred from the analysis of the strike of the longitudinal normal faults, as well as to locate elements responsible for their formation within the overlying thrust sheets by examining the available geological maps.

3.3. Stratigraphy

The normal faults studied here involve the following stratigraphic units, listed from oldest to youngest: Rañeces Gr., Moniello Fm., Alba Fm. and Barcaliente Fm.

In the studied outcrops, the Rañeces Gr. consists of ochre-coloured sandstones and slates with sporadic centimetre-scale levels of black slates, as well as grey limestones with intercalations of ochre-grey marls and black slates (e.g., García Fuente, 1952, 1953; Almela et al., 1956; Pello Muñíz et al., 1976; Bulnes, 1989, 1995; Bulnes et al., 1999) (Figs. 8 and 9). Its age, based on its fossil content, is Lower Devonian (Vera de la Puente, 1989). The more resistant layers of this unit, where the faults under study are better developed, are the limestones; they have supplied Schmidt-hammer rebound values of almost 40 (Table 2).

The Moniello Fm., in the studied outcrops, comprises grey limestones with birdseyes, and sporadic interbeds of slates and reddish-grey marls (e.g., Martínez-Álvarez et al., 1975; Bulnes, 1989, 1995) (Figs. 10 and 11). This stratigraphic unit has been assigned to the Lower-Middle Devonian based on its fossil content (e.g., Barrois, 1882; Méndez-Bedia, 1976). The limestones exhibit Schmidt-hammer rebound values ranging from almost 50 to almost 60 (Table 2).

In the studied outcrops, the Alba Fm. is composed of a lower part consisting of red, nodular limestones (griotte facies) with scarce red slate interbeds. The middle part contains alternations of red to grey radiolarites and red, grey-greenish, and beige siliceous slates. The upper part consists of red, nodular limestones (griotte facies) and grey limestones interbedded with red and grey-greenish slates, transitioning to light grey limestones with occasional grey-greenish slate interbeds up section (e.g., Martínez-Álvarez et al., 1975; Pello Muñíz et al., 1976; Rodríguez-Fernández et al., 1991; Bulnes et al., 2016, 2019) (Fig. 12). Its age, determined based on its fossil content and U-Pb dating of volcanic ash layers, is Mississipian (e.g., Adrichem Boogaert, 1965; Merino-Tomé et al., 2017). The limestone layers are the most competent rocks where the faults are better developed; these show Schmidt-hammer rebound values slightly higher than 60 (Table 2).

The Barcaliente Fm., in the studied outcrops, is composed of dark grey to black limestones, some of which are laminated, with intercalated marly limestones (e.g., Rodríguez-Fernández and Navarro Vázquez, 1982; Leyva et al., 1984; Poblet et al., 2022) (Fig. 13). Although this stratigraphic unit has not been directly dated, it is considered to have a Carboniferous age, including the Mississipian-Pennsylvanian boundary, based on the ages of the underlying and overlying stratigraphic units. The limestone layers, which are the most competent and where the faults are better developed, display Schmidt-hammer rebound values ranging from almost 50 to slightly more than 60 (Poblet et al., 2022) (Table 2).

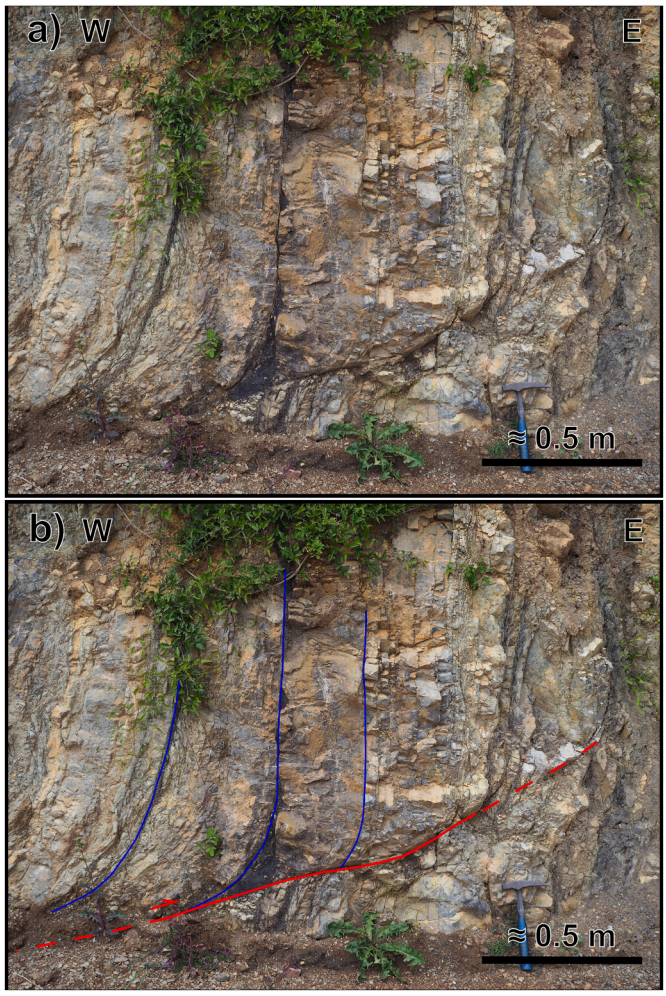

Fig. 8. a) Photograph and b) photogeological interpretation of a tilted normal fault and a related drag fold in the Bandujo outcrop (Devonian Rañeces Gr.). Blue lines: bedding, red line: normal fault. See Figs. 3 and 15 for location. (For interpretation of the references to colour in this figure legend, the reader is referred to the Web version of this article.)

3.4. Normal faults

3.4.1. Main structural features

The studied faults are not very common. They exhibit variable orientations within the same locality, as well as across different localities, transitioning from NE-SW to N-S to NW-SE and to E-W strikes, with variable dips ranging from subhorizontal to moderate in different directions (Fig. 14). When these faults involve subhorizontal layers, they are normal faults; however, when they involve steeply dipping beds, they appear to be reverse faults (Figs. 8–12). Nevertheless, when the stratification is rotated to the horizontal and the faults rotated accordingly, all of them become normal faults and acquire dips from approximately 65 to 75° (Fig. 15).

Most faults are planar and do not cause rotation of the layers, and both the hangingwall and the footwall rocks display a ramp disposition relative to the faults (Figs. 8–13). However, listric faults have occasionally been identified, with detachments located within incompetent rocks, such as slates. These listric faults give rise to gentle rollovers (Fig. 9). A few faults exhibit associated drag folds, with the limb adjacent

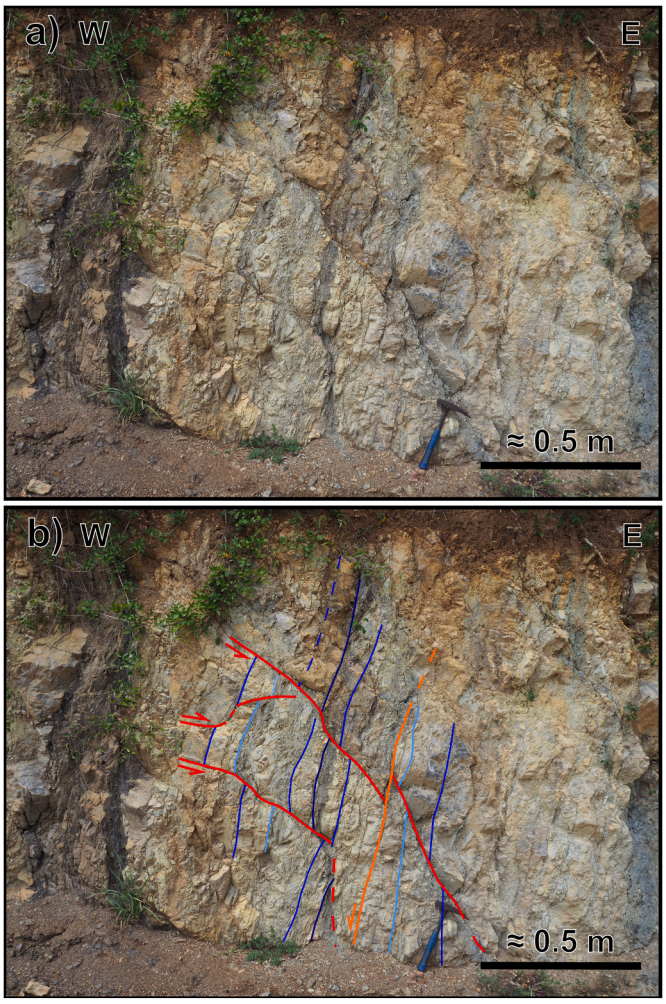

Fig. 9. a) Photograph and b) photogeological interpretation of a tilted listric normal fault and of a tilted normal fault cut and offset by a bedding surface, whose motion is consistent with flexural slip, in the Bandujo outcrop (Devonian Rañeces Gr.). Blue lines: bedding, red lines: normal faults, orange line: flexural-slip surface. See Figs. 3 and 15 for location. (For interpretation of the references to colour in this figure legend, the reader is referred to the Web version of this article.)

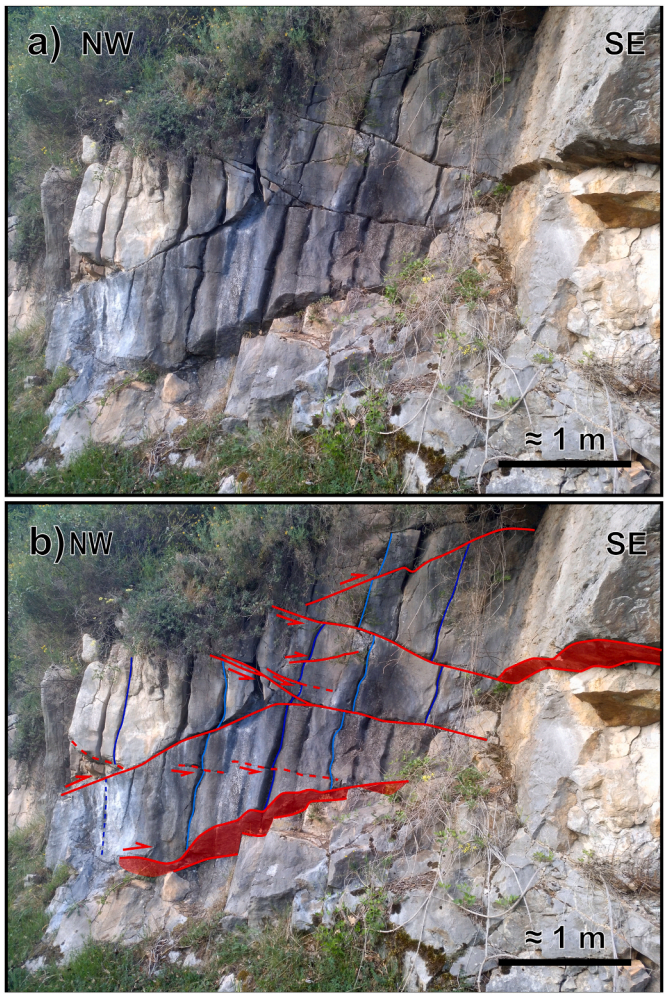

Fig. 10. a) Photograph and b) photogeological interpretation of tilted conjugate normal faults in the Baselgas outcrop (Devonian Moniello Fm.) where the maximum fracturing areal intensity has been obtained. Blue lines: bedding, red lines: normal faults. See Figs. 3 and 15 for location. (For interpretation of the references to colour in this figure legend, the reader is referred to the Web version of this article.)

Table 2
Average Schmidt-hammer rebound values and fracture intensity values for different stratigraphic units obtained in different studied outcrops.

AGE	STRATIGRAPHIC UNIT	LITHOLOGY	AVERAGE SCHMIDT-HAMMER REBOUND VALUES + OUTCROP	FRACTURE INTENSITY VALUES + OUTCROP
Carboniferous	Barcaliente Fm.	Black limestones	47.5–62.5 (Vega de los Viejos)	2 m^{-1} (Vega de los Viejos)
Carboniferous	Alba Fm.	Red limestones	61.5 (Tellego)	1 m^{-1} (San Emiliano)
Devonian	Moniello Fm.	Grey limestones	47.0–57.5 (Baselgas)	3 m^{-1} (Baselgas)
Devonian	Rañeces Gr.	Grey limestones	39.0 (Linares)	3 m^{-1} (Bandujo)

to the fault showing moderate dips. The asymmetry of these folds is consistent with normal fault motion when bedding is rotated to the horizontal and the faults rotated accordingly (Fig. 8). Relay ramps between normal faults have been occasionally identified. The surfaces of these faults can be either smooth or rough; in the latter case, small rock fragments may remain along the fault, surrounded by it (Fig. 11). These faults exhibit a metre-scale or smaller size, and produce maximum displacements of the layers in the centimetre-decimetre range. In some outcrops, we have observed that the offset along a fault, which is maximum in its central part, progressively decreases until it becomes null at its upper and lower tips (Fig. 12). The fault displacement accommodation in fault terminations can occur as gentle folds affecting the layers where faults tip are located or as fractures and veins very close to the fault tips (Fig. 11). Three types of kinematic criteria have been identified on the fault surfaces, although they are extremely rare: fault striations, fault slickensides and small calcite-filled pull-aparts. All the criteria indicate that they are dip-slip faults.

In many outcrops, two families, forming a conjugate system, are observed (red lines in the photogeological interpretations in Figs. 10 and 12, and red lines in the equal-area projections in Fig. 15). This conjugate fault system is responsible for small horsts and grabens, such that neither family predominates over the other. The acute angle of the conjugate

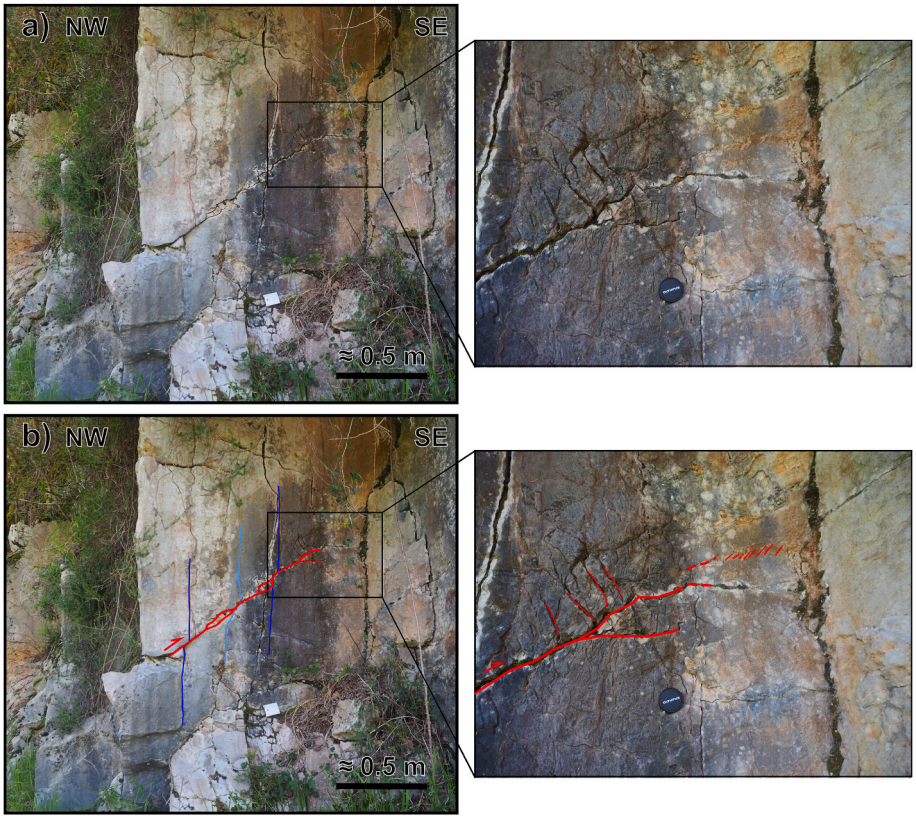

Fig. 11. a) Photograph and b) photogeological interpretation of a tilted normal fault and zoom of its lower tip in the Baselgas outcrop (Devonian Moniello Fm.). Blue lines: bedding, red line: normal fault. See Figs. 3 and 15 for location. (For interpretation of the references to colour in this figure legend, the reader is referred to the Web version of this article.)

fault system ranges from approximately 30 to 50°. In some outcrops, such as the ones near Vega de Los Viejos and San Emiliano, after rotating bedding and faults, four fault families can be identified. Two of these families form the conjugate fault system mentioned above (red lines in the equal-area projections in Fig. 15), while the other two form a different conjugate system (green lines in the equal-area projections in Fig. 15). These two conjugate fault systems are approximately perpendicular to each other. The temporal relationships between the two conjugate fault systems have not been established because cross-cutting or other type of criteria are lacking.

The main criteria employed to group all these faults as part of the same deformation event is not their orientation, which as described above is variable, but rather other parameters such as their normal kinematics in regions where bedding is subhorizontal or once bedding has been rotated to the horizontal, their similar characteristics in terms of frequency, geometry, dimensions, displacement, and conjugate fault systems, and especially their age, which is described below.

3.4.2. *Timing of the normal faults*

The structure of the regions where these normal faults have been mapped consists mainly of folds and thrusts, which can reach kilometric dimensions and displacements. Their orientation varies from NE-SW in the northern part of the study area to N-S in the central part, to E-W in the southern part (Figs. 3 and 15). A spaced cleavage, whose orientation is consistent with that of the folds, has been locally recognized; it could be interpreted either as an axial-plane cleavage or as a cleavage resulting from layer-parallel shortening in the initial stages of fold development. These structures have been described in the study area by Pello Muñiz (1974), Martínez-Álvarez et al. (1975), Pello Muñíz et al. (1976), Rodríguez-Fernández and Navarro Vázquez (1982, 1991), Bastida et al. (1984), Leyva et al. (1984), Alonso et al. (1989), Bastida and Gutiérrez (1989), Bulnes (1995), Bulnes and Marcos (2001) and Bulnes and Aller (2002) amongst others.

Based on the following criteria, we conclude that the normal faults developed prior to the folds and thrusts.

i) There are normal faults cut and offset by thrust faults. In some cases, such as in Fig. 12, thrust faults may be tilted by folds developed during later stages.
ii) There are normal faults cut and offset by bedding surfaces that underwent flexural slip consistent with the folds (Fig. 9). The fault slickensides indicating flexural slip, developed on the bedding surfaces, are approximately perpendicular to the fold axes and the motion sense along the bedding surfaces is consistent with the expected motion in flexural-slip anticlines and synclines.
iii) There are hangingwall anticlines adjacent to normal faults, interpreted as a result of buttressing (Fig. 13). The fault displacement of a reference horizon indicates normal faulting; however, the same reference horizon at the crest of the anticline adjacent to the fault is located at a higher elevation than the regional elevation defined for the same horizon. This points out that the normal faults were prior to the development of the folds.
iv) There are tilted conjugate normal faults in fold limbs (Figs. 8–12). Since the bedding surfaces approximately bisect the obtuse angle between the conjugate normal faults, the faults acquire an almost symmetrical arrangement when the bedding is placed in a horizontal position. The fact that bedding bisects the obtuse angle between the normal faults suggests that these faults developed when bedding was horizontal, and therefore, it indicates that normal faulting predates folding.
v) There are normal faults on both limbs of the same fold (Fig. 14d and e, 14j and 14k, and 14l and 14m) that acquire the same orientation once, using the fold axis, the layers are rotated to a

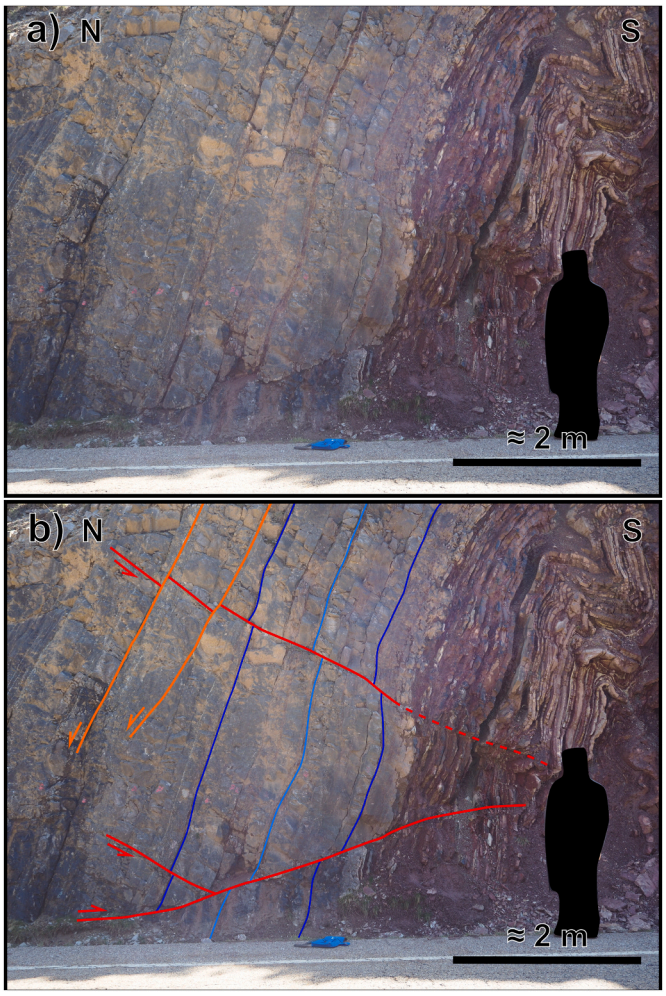

Fig. 12. a) Photograph and b) photogeological interpretation of tilted conjugate normal faults in the San Emiliano N outcrop (Carboniferous Alba Fm.) cut and offset by tilted thrust faults slightly oblique to bedding. Blue lines: bedding, red lines: normal faults, orange lines: thrust faults. See Figs. 3 and 15 for location. (For interpretation of the references to colour in this figure legend, the reader is referred to the Web version of this article.)

horizontal position and the normal faults are rotated accordingly (Fig. 15). This points out that the normal faults developed before folding.

vi) Some normal faults are folded.

vii) There are fold-related cleavage surfaces developed in one of the normal fault blocks that terminate against the normal fault surface. Considering the offset caused by the fault, these cleavage surfaces do not appear where they should be expected to occur in the other fault block. Therefore, we conclude that the cleavage surfaces are not offset by the fault, but abut it. This points out that the normal fault predates cleavage, and therefore, folding.

In some outcrops, only one of the aforementioned criteria has been identified, while in others, more than one criterion has been recognized. For example, tilted conjugate normal faults cut and offset by thrust faults been observed at the San Emiliano N outcrop (Fig. 12), normal faults cut and offset by flexural slip and affected by buttressing phenomena have been identified at the Vega de los Viejos N outcrop, and tilted conjugate normal faults and fold-related cleavage surfaces that abut against normal fault surfaces has been observed at the Baselgas outcrop (Figs. 10 and 11). No normal faults reactivated as reverse faults have been recognized in any of the outcrops.

The studied normal faults cut and offset Devonian and Mississipian rocks. The thickness of the layers offset by the faults is approximately the same in the hangingwall and in the footwall, indicating no growth faulting, i.e., no syn-extensional sedimentation (Figs. 8–13). Therefore, we conclude that the faults developed after the deposition of the Devonian and Mississipian rocks. The syntectonic sediments and the unconformities mapped in the southern part of the Cantabrian Zone led Alonso (1987) to assign a Pennsylvanian age to some contractional structures. Thus, since the normal faults postdate the youngest rocks cut and offset by them, and predate the contractional structures, their age may be constrained during the lower part of the Pennsylvanian.

3.4.3. *Origin of the normal faults*

At first glance, some faults developed on the dipping limbs of the folds, which currently exhibit an apparent reverse movement (Figs. 8–12), may be interpreted as fold-related thrusts. However, as previously mentioned, some of these faults are cut and offset by bedding surfaces that have undergone flexural slip related to the folds, some of them are a barrier for the development of fold-related cleavage surfaces, and some of them are folded, pointing out that these faults predate the folds. In addition, the conjugate faults acquire an approximately

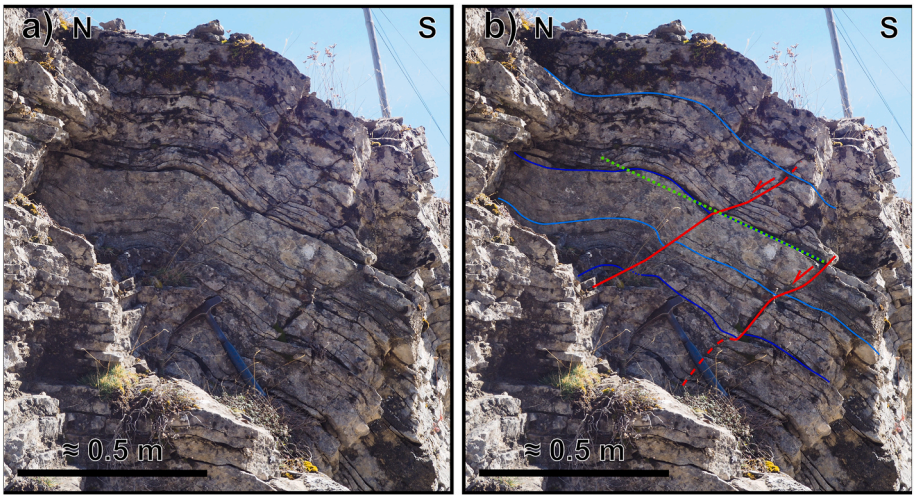

Fig. 13. a) Photograph and b) photogeological interpretation of a fold formed by buttressing in relation to a normal fault in the Vega de los Viejos N outcrop (Carboniferous Barcaliente Fm.). Blue lines: bedding, red lines: normal faults, green line: regional of a bedding surface. See Figs. 3 and 15 for location. (For interpretation of the references to colour in this figure legend, the reader is referred to the Web version of this article.)

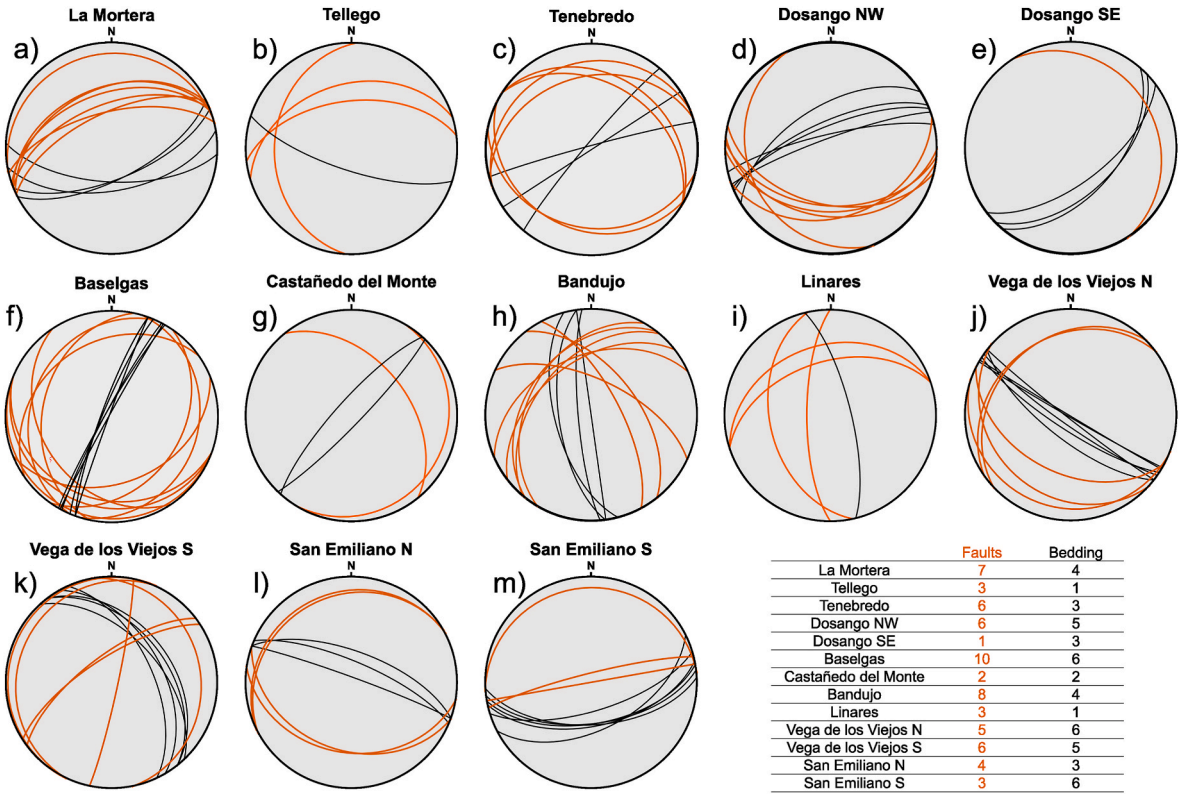

	Faults	Bedding
La Mortera	7	4
Tellego	3	1
Tenebredo	6	3
Dosango NW	6	5
Dosango SE	1	3
Baselgas	10	6
Castañedo del Monte	2	2
Bandujo	8	4
Linares	3	1
Vega de los Viejos N	5	6
Vega de los Viejos S	6	5
San Emiliano N	4	3
San Emiliano S	3	6

Fig. 14. Equal-area projections of the normal faults (orange lines) and bedding (black lines) measurements taken in the studied outcrops. The number of measurements plotted in each projection are listed in the table. See Figs. 3 and 15 for location of the outcrops. (For interpretation of the references to colour in this figure legend, the reader is referred to the Web version of this article.)

symmetrical arrangement when bedding is placed in a horizontal position indicating that they were formed when bedding was approximately horizontal (Fig. 15). Moreover, the fact that some normal faults are oblique to the fold limbs, and that families of faults with similar orientations have been mapped in some outcrops, such as the San Emiliano and the Vega de los Viejos outcrops (Fig. 14), despite that the folds responsible for their tilting have different trends, indicate that the normal faults and folds are unrelated.

We interpret that most of these normal faults are old longitudinal flexural normal faults related to the footwall flexure caused by the fold-and-thrust belt during its advance towards the foreland. The following arguments support this hypothesis. When bedding is restored to a horizontal position and the faults are rotated accordingly, they become normal faults and the strike of most of them is perpendicular or oblique to the available data on the tectonic transport direction of the overlying thrust sheets determined by Gutiérrez Alonso (1992), Bulnes (1995), Bulnes and Marcos (2001), Caldera Grau (2016) and de Paz Álvarez (2023) (Fig. 15). In addition, the faults are prior to the thrusts and folds, and formed when bedding was horizontal in the layers within the pre-Variscan stratigraphic succession (Figs. 9–13). Moreover, the normal faults are much less abundant and are shorter than the folds and thrusts, and exhibit small displacements, which points out that they derive from small extension values. Those normal faults that exhibit the same characteristics as those described above, except that once rotated their strike is approximately parallel to the tectonic transport vectors (Fig. 15), have been interpreted as transverse normal faults. Their precise origin will be discussed later.

We cannot rule out that the normal faults studied here might belong to an ancient extensional event prior to the development of the fold-and-thrust belt. Nevertheless, if they were normal faults related to an ancient extensional event that took place prior to any other deformation, it is very likely that the resulting normal faults would have developed with an approximately consistent orientation. If that were the case, once incorporated into the fold and thrust belt, they would have maintained a constant angular relationship with the contractional tectonic transport vectors throughout the region. However, this is not the case. Moreover, no extensional events older than the Variscan contractional event have been described in the study area.

3.5. *Orogenic front trend, thrust propagation sequence, flexure tightness, oblique/lateral structures and uncertainties*

3.5.1. *Trend of the fold-and-thrust belt front*

Once rotated to their initial attitude, the strikes of the longitudinal flexural normal faults show the orientation of the fold-and-thrust belt front, i.e., the Cantabrian Zone front, when their overlying thrust sheets were the frontal ones. The old orogenic fronts shift from E-W and NE-SW in the northern branch of the Ibero-Armorican (or Asturian) Arc, to N-S in the central part, to NW-SE in the southern branch, so that a large variation is observed from north to south. This pattern outlines the core of the Ibero-Armorican or Asturian Arc (Figs. 3 and 15).

The strikes of the longitudinal normal faults mapped form an angle comprised between 90° and 30° with the tectonic transport vectors obtained from their overlying thrust sheets (Figs. 15 and 16a). In the southern branch of the Ibero-Armorican Arc, where the tectonic transport vectors display a NE-SW direction, the angle between the strike of the longitudinal normal faults and the tectonic transport vectors ranges from 90° to approximately 75°. However, in the northern branch of the Arc, where the tectonic transport vectors exhibit a WNW-ESE direction, the angles between the strike of the normal faults and the tectonic transport vectors range from approximately 65 to 30° (Figs. 15 and 16a).

In order to better visualize the shape of the orogenic fronts in the past, the tectonic transport vectors used for the studied outcrops have been rotated around a vertical axis so that all of them share a N040°E

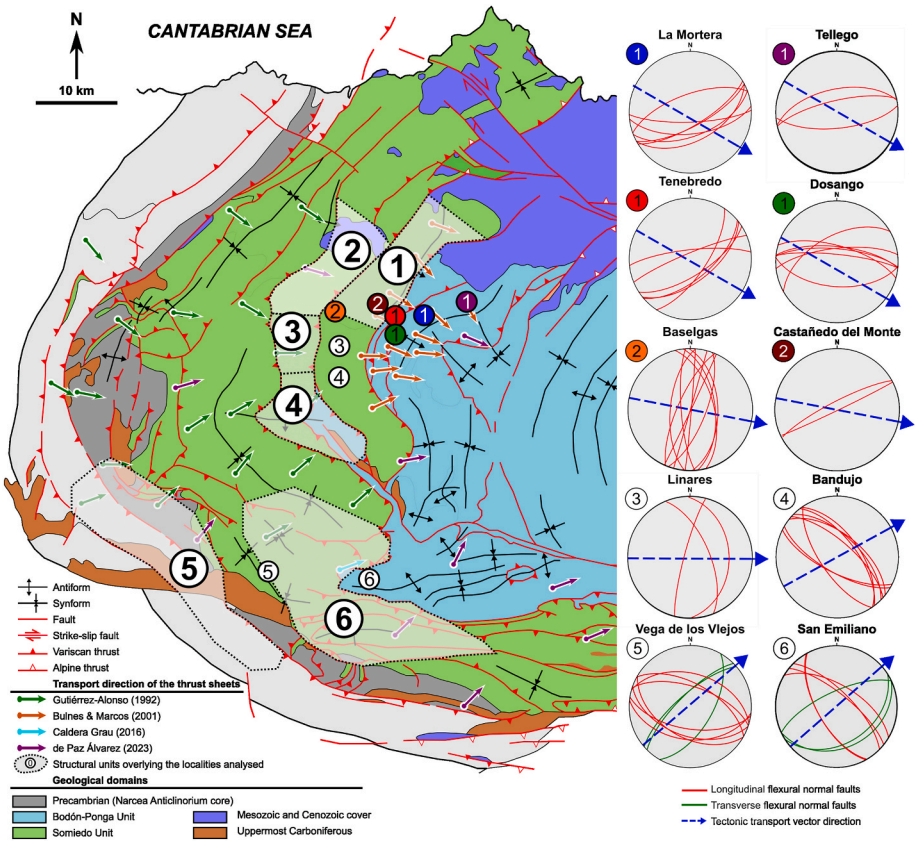

Fig. 15. Structural sketch of the western part of the Cantabrian Zone (modified from Alonso et al., 2009a) including tectonic transport vectors plotted by De Paz Álvarez (2023) collected from different authors. The equal-area projections of each studied outcrop show the normal faults rotated to their original attitudes (red and green lines) and the tectonic transport vector obtained from the overlying structural unit (blue arrow). (For interpretation of the references to colour in this figure legend, the reader is referred to the Web version of this article.)

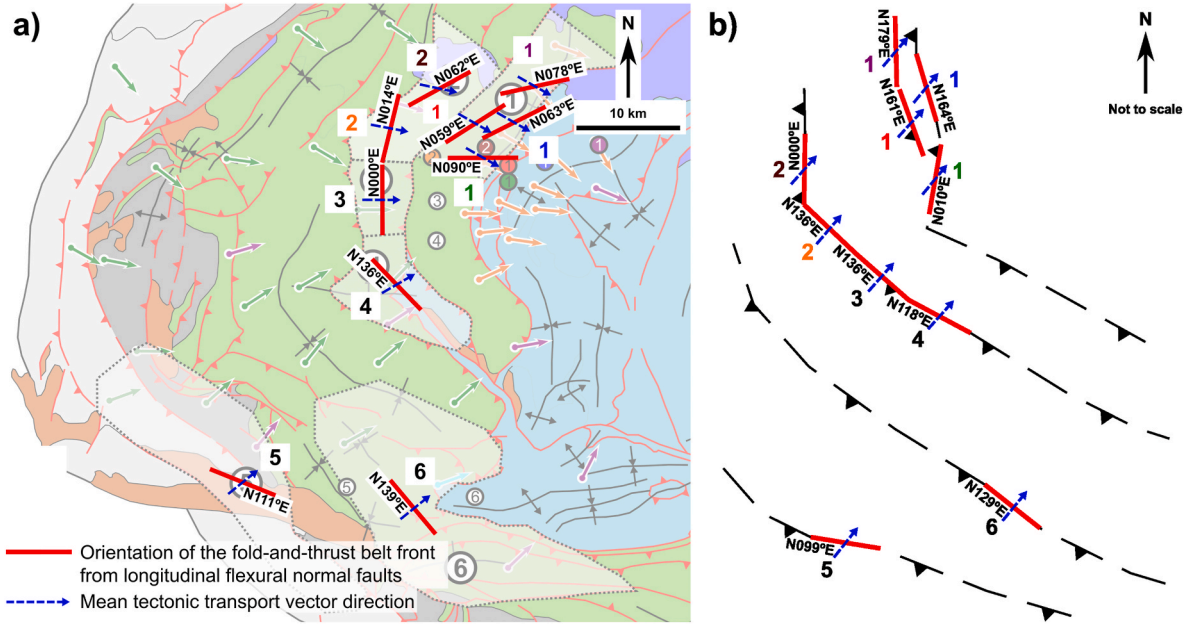

Fig. 16. a) Structural sketch of a portion of the western part of the Cantabrian Zone (modified from Alonso et al., 2009a) including the traces of the fold-and-thrust belt front in the studied outcrops resulting from the analysis of longitudinal flexural normal faults, as well as tectonic transport vectors obtained from the literature. Same legend as in Fig. 15 b) Structural sketch of the western part of the Cantabrian Zone once all the tectonic transport vectors in the studied outcrops have been rotated to N040°E along with the traces of the fronts of the fold-and-thrust belt.

orientation, and the traces of the orogenic fronts have been rotated accordingly (Fig. 16b). This orientation of the reference tectonic transport vector has been adopted following the reconstruction of De Paz Álvarez (2023). Although the available data are limited—since the primary objective of this article is to demonstrate the usefulness of studying flexural normal faults and applying this approach to some outcrops in the Cantabrian Zone—the results obtained point out that the belt front was more rectilinear and more perpendicular to the tectonic transport vector in the southern branch of the Arc, where the maximum angle between the strike of different portions of the orogenic front is 15°, than in the northern one, where the angle is 35°. The angle between the trend of the longitudinal flexural normal faults and the tectonic transport vector, as well as the reconstruction depicted in Fig. 16b, show that the ancient orogenic front was more advanced toward the foreland in the northern branch than in the southern one. De Paz Álvarez (2023) obtained a similar thrust configuration by using a different method which consisted of rotating the axial traces of folds related to frontal ramps.

3.5.2. *Thrust propagation sequence*

The normal faults identified in all the studied outcrops, located in different thrust sheets, predate the folds and thrusts (Figs. 8–13). This means that each new thrust sheet developed on a previously flexed and normal faulted footwall. Thus, this is diagnostic of a forward-breaking or "piggy-back" thrust propagation sequence. The thrust emplacement sequence deduced here is consistent with that inferred by Pérez-Estaún et al. (1988), Pérez-Estaún and Bastida (1990) and Aller et al. (2004), among others, using criteria such as the age of syn-tectonic strata and cross-cutting relationships between contractional structures.

3.5.3. *Flexure curvature, dip of the flexure inclined limb and flexure interlimb angle*

Many limestones studied here exhibit relatively similar Schmidt-hammer rebound values. Thus, the measurements of fracturing intensity carried out at different outcrops are more or less comparable. The maximum fracturing areal intensity due to longitudinal flexural normal faults is approximately 3 m^{-1} and has been obtained in the Baselgas outcrop, located in the north branch of the Ibero-Armorican or Asturian Arc, made up of Moniello Fm. limestones (Table 2 and Fig. 10). The fracturing areal intensity estimated in other outcrops is lower. These low values suggest that both the flexure curvature and the dip of the flexure inclined limb were very gentle, and that the flexure interlimb angle was very high when these normal faults were formed. These low numbers might also suggest that the weight of the fold-and-thrust belt was relatively low. This conclusion makes a lot of sense considering that the analysed normal faults occur in thrust sheets that belong to the western part of the foreland fold-and-thrust belt. In other words, these thrust sheets are relatively far from the foreland and, therefore, when they were emplaced, the fold-and-thrust belt was still at an intermediate stage, with several thrust sheets yet to be emplaced eastwards.

3.5.4. *Oblique/lateral thrust structures*

Once the stratification has been rotated to a horizontal position, along with the faults, the San Emiliano and Vega de los Viejos outcrops, all located in the southern branch of the Ibero-Armorican Arc, reveal the occurrence of two systems of conjugate normal faults with different strikes. These faults are: faults perpendicular and oblique to the tectonic transport vectors of the overlying thrust sheets, i.e., longitudinal faults (red lines in the equal-area projections in Fig. 15), and faults approximately parallel to the tectonic transport vectors, i.e., transverse faults (green lines in the equal-area projections in Fig. 15). Transverse faults have not been recognized in the rest of studied outcrops.

To look for the cause of the transverse normal faults in the San Emiliano outcrops we have examined the geological features of their overlying thrust sheet in the available geological maps (e.g., Bastida et al., 1984; Alonso et al., 1989; Suárez-Rodríguez et al., 1988–89; Instituto Geológico y Minero de España, 2021). The thrust sheet that overlies the San Emiliano outcrops is called Somiedo (green units in the map depicted in Fig. 17). This thrust sheet includes an ENE-WSW lateral ramp, of more than 10 km length, that places the Aralla-Rozo thrust slice to the southeast over the Villar-Robledo thrust slice to the northwest (Alonso et al., 1989), causing an abrupt and significant along-strike change in the internal structure of this thrust sheet. Three points, based on the spatial position and orientation of the lateral ramp and of the transverse faults, suggest a possible genetic relationship between both structural elements.

i) A hypothetical prolongation of the lateral ramp towards the northeast runs across the studied San Emiliano outcrops (see the map in Fig. 17), i.e., the spatial position of both the lateral ramp and the transverse faults is consistent.
ii) The lateral ramp trace on the geological map trends approximately N065°E, while the strike of a bisector plane of the conjugate transverse normal faults in the San Emiliano outcrops is approximately N045°E (Fig. 15), i.e., the directions of the lateral ramp and transverse faults are relatively coincident.
iii) The transverse normal faults described only appear in the San Emiliano S outcrop (Figs. 14 and 17). According to the direction and motion sense of the tectonic transport vector of the overlying thrust sheet, i.e., the Somiedo thrust sheet (Fig. 17), as well as the orogenic front trend deduced from these outcrops (Fig. 16b), the San Emiliano S outcrop was closer to the fold-and-thrust belt front, and therefore, to the lateral ramp of the Somiedo thrust sheet, than the San Emiliano N outcrop.

Thus, we propose that these transverse normal faults in the San Emiliano outcrops are flexural normal faults related to an old transverse foredeep flexure, not preserved nowadays. This transverse foredeep flexure would have been caused by the presence of the lateral ramp in the Somiedo thrust sheet, when it was the frontal thrust sheet of the Cantabrian fold-and-thrust belt. The proximity of the transverse normal faults to the lateral ramp is consistent with the fact that transverse flexures caused by lateral ramps are usually smaller in scale than longitudinal flexures parallel to the front of fold-and-thrust belts.

In an attempt to deduce the cause responsible for the transverse normal faults in the Vega de los Viejos outcrops, we have examined the geological features of the overlying thrust sheet, called Narcea. To the south and west of the studied outcrops, detrital rocks and coals from the uppermost Pennsylvanian (Stephanian) (brown rocks in the maps depicted in Figs. 1, 3 and 15,16a and 17), deposited after the Variscan orogeny climax, lay unconformably on a portion of the Narcea thrust sheet (e.g., Navarro Vázquez and Rodríguez-Fernández, 1982; Bastida et al., 1984; Alonso et al., 1989; Instituto Geológico y Minero de España, 2021) preventing its internal structure from being properly observed. However, there are two arguments supporting an important along-strike change within the Narcea thrust sheet.

i) According to Alonso et al. (2009b), south of the Stephanian deposits, there is a single main thrust within the Narcea thrust sheet, while to the north of these deposits, there are two main thrusts (thrusts within the Precambrian rocks—pink colour—in the map depicted in Fig. 3).
ii) According to the geological maps constructed by Alonso et al. (1989) and Instituto Geológico y Minero de España (2021) the width of the Narcea thrust sheet is considerably greater to the north of the Stephanian deposits than to the south (Figs. 3 and 17).

These along-strike variations of the Narcea thrust sheet may be due to the occurrence of an oblique ramp. Thus, the Stephanian deposits are bounded to the south-southwest by a fault that also involves the pre-Variscan succession (e.g., Navarro Vázquez and Rodríguez-Fernández, 1982; Bastida et al., 1984; Alonso et al., 1989; Instituto Geológico y Minero de España, 2021). Part of this fault is oblique to the strike of the Variscan structures, but it seems to follow the strike of the Variscan

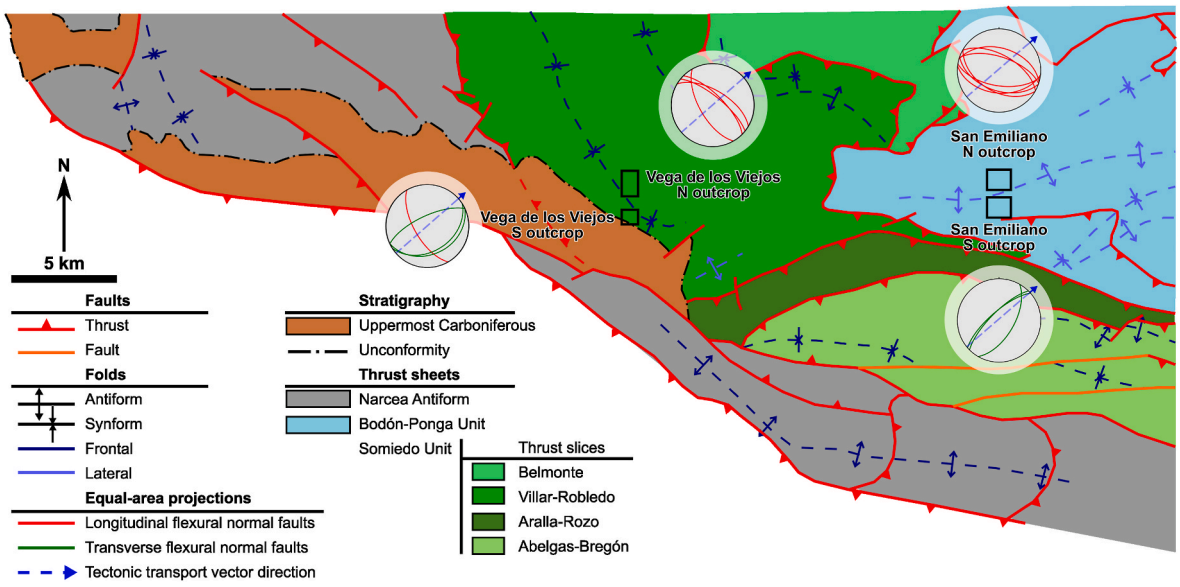

Fig. 17. Geological map of the southwestern part of the Cantabrian Zone (modified from Alonso et al., 1989), showing the lateral ramp responsible for overthrusting the Aralla-Rozo slice on the Villar-Robledo slice, both located in the Somiedo thrust sheet overlying the San Emiliano outcrops, and the oblique ramp within the Narcea thrust sheet overlying the Vega de los Viejos outcrops. The black rectangles show the location of the San Emiliano N, San Emiliano S, Vega de los Viejos N and the Vega de los Viejos S outcrops. The equal-area projections of these outcrops show the longitudinal and transverse normal faults, once rotated to their original attitudes, and the tectonic transport vectors of their overlying thrust sheets.

structures both to the northwest and to the southeast (Instituto Geológico y Minero de España, 2021) (Fig. 17), suggesting that it might have been a Variscan oblique thrust ramp, of approximately 30 km length, later on reactivated. Similarly to the San Emiliano outcrops, the transverse normal faults appear only in the Vega de los Viejos S outcrop (Figs. 14 and 17). According to both the direction and motion sense of the tectonic transport vector of the overlying thrust sheet, i.e., the Narcea thrust sheet (Fig. 17), as well as the trend of the fold-and-thrust belt front deduced from these outcrops (Fig. 16b), the Vega de los Viejos S outcrop was closer to the fold-and-thrust belt front and to the oblique ramp of the overlying thrust sheet, than the Vega de los Viejos N outcrop. This supports a possible genetic relationship between the transverse normal faults and the oblique ramp.

Thus, we propose that the transverse normal faults in the Vega de los Viejos outcrops may be flexural normal faults related to an old transverse foredeep flexure, probably overprinted by the contractional structures. This flexure was caused by the described oblique ramp in the overlying Narcea thrust sheet when it was located at the frontal part of the fold-and-thrust belt. Again, the proximity of the transverse normal faults to the lateral ramp supports the hypothesis that transverse flexures produced by oblique structures are smaller than longitudinal flexures parallel to the fold-and-thrust belt front.

3.5.5. *Influence of the Ibero-Armorican Arc closure, Permian-Mesozoic extension and Cenozoic (Alpine) contraction on the Variscan orogenic front directions, thrust propagation sequence and oblique/lateral thrust structures*

Some studies have suggested that the closure of the Ibero-Armorican or Asturian Arc, which occurred by the end of the Palaeozoic, led to the formation of all or part of the so-called radial folds or to the reactivation of previous lateral folds, resulting in fold interference patterns, and even to the reactivation of thrust surfaces in various localities of the Cantabrian Zone (e.g., Julivert, 1971; Julivert and Marcos, 1973; Julivert and Arboleya, 1984; Pérez-Estaún et al., 1988; Van der Voo et al., 1997; Weil et al., 2000).

Studies on the characteristics of the Permian-Mesozoic extensional events that affected the Cantabrian Zone have been primarily conducted in the northern portion of the Cantabrian Mountains, as it is where most post-Variscan rocks affected by these events crop out unconformably over the Variscan basement. These extensional tectonics events resulted in a set of faults distributed throughout the region, some of which likely resulted from the reactivation of faults inherited from the Variscan cycle. Most faults exhibit relatively small vertical displacements (e.g., Lepvrier and Martínez García, 1990; Uzkeda, 2013; Odriozola, 2016; Uzkeda et al., 2016, 2025; Magán, 2017, 2024), although a few ones reached larger vertical displacements around a few hundred meters (e.g., Alonso et al., 2016; Uzkeda et al., 2025).

Regarding the effects of the Alpine orogeny of Cenozoic age, in the northern part of the Cantabrian Mountains, where post-Variscan rocks have been preserved, reverse faults and strike-slip faults with generally small displacements, as well as open folds, have been documented (e.g., Lepvrier and Martínez García, 1990; Uzkeda, 2013; Alonso López, 2014; Odriozola, 2016; Uzkeda et al., 2016, 2025; Magán, 2017, 2024; Magán et al., 2022). However, some faults reach vertical displacements of around 0.5 km (Alonso et al., 1996, 2009a; Pulgar et al., 1999). A crustal scale section across the Cantabrian Mountains reveals a frontal thrust ramp at depth with a dip of approximately 15°, involving almost the entire Cantabrian Mountains except for its northern margin. This thrust ramp caused maximum uplifts slightly exceeding 5 km according to the geological cross-sections depicted in Alonso et al. (1996, 2009a) and Pulgar et al. (1999). At the southern edge of the Cantabrian Mountains, near its boundary with the Alpine foreland basin, a frontal anticline related to the deep thrust ramp developed, accommodating about 10 km of displacement. This fold caused a noticeable southwards rotation of the Variscan structures, along a subhorizontal approximately E-W axis (Alonso et al., 1996, 2009a; Pulgar et al., 1999). The degree of Alpine reactivation of the Variscan structures developed in Palaeozoic rocks depends on the angle they form relative to the major principal axis (σ1) of the Alpine stress field, which in this region is approximately N-S (Lepvrier and Martínez García, 1990; Uzkeda, 2013; Uzkeda et al., 2025). Thus, some Variscan structures striking E-W, i.e., approximately perpendicular to the direction of maximum Alpine compressive stress, accommodated Alpine shortening through fold tightening as well as thrust reactivation and verticalization (Pulgar et al., 1999). Some Variscan thrusts and other faults with NE-SW and NW-SE trends were reactivated as oblique-slip faults or strike-slip faults during the Alpine

orogeny. The Alpine shortening, irregularly distributed within the Palaeozoic rocks, has been estimated to reach a value of approximately 20 % (Pulgar et al., 1999).

In the outcrops analysed here, no significant folds, nor faults, have been identified whose development could be unequivocally attributed to the Ibero-Armorican Arc closure, Permian-Mesozoic extension and/or to the Cenozoic contraction. Only one structure, briefly described below, deserves to be mentioned. In the San Emiliano N outcrop, a thrust fault has been identified whose orientation and layer displacement are consistent with the Variscan structuring of the outcrop and its surroundings. However, the thrust surface exhibits slickensides not compatible with the layer displacement (Masini et al., 2010a; Bulnes et al., 2019). It is highly likely that this thrust fault was reactivated during the Ibero-Armorican Arc closure, the Permian-Mesozoic extension and/or the Cenozoic contraction. We believe this structure has not exerted sufficient influence to warrant consideration when rotating the stratification and the normal faults to determine their original attitude. This is because the reactivation has been minor, insufficient to, for instance, counteract the Variscan reverse offset and convert the thrust into a different type of fault. The fact that rotating the normal faults yields results consistent with the tectonic transport vector of the overlying Variscan thrust sheet appears to support this assumption.

It is possible that some Variscan folds observed in different outcrops were tightened and that some Variscan thrust surfaces were reactivated during the Ibero-Armorican Arc closure and/or Alpine contractional event. Therefore, while the cross-cutting relationships between folds and thrusts and normal folds presented here are coherent, these might have been influenced by these younger events. Nevertheless, the fact that the conjugate faults become normal faults with nearly symmetrical positions when the stratification is rotated to horizontal—indicating that they formed before any tilting of the stratification—and that rotating the normal faults to their original attitude when the stratification was horizontal yields results consistent with the direction of tectonic transport vectors of the thrust sheets in this region, gives us confidence in the observations made and the procedures applied. Thus, we believe the post-Variscan structures have no clear influence on determining the directions of the Variscan orogenic front, the propagation sequence of Variscan thrust sheets and the presence of oblique/lateral structures.

4. Conclusions

The load caused by the advance of a fold-and-thrust belt towards the foreland induces a foredeep flexure. We propose that this flexure amplifies due to a combination of hinge migration and limb rotation, and that its hinge zone undergoes tangential longitudinal strain. These mechanisms cause the development of longitudinal flexural normal faults in the hinge zone that are progressively incorporated into the flexure inclined limb as the active axial surface migrates relative to the rocks. Additionally, the original arcuate shape of the fold-and-thrust belt, as well as the presence of lateral/oblique structures, can lead to the development of transverse normal faults. The main criteria to recognize flexural normal faults and differentiate them from other types of normal faults, especially when they formed in the early or intermediate stages of the fold-and-thrust belt development, are their relative timing with respect folds and thrusts, their angular relationship with bedding, their fault kinematics, their slip/frequency/length compared to those of the folds and thrusts, the age of the rocks cut and offset by the normal faults, the angle between the strike of the normal faults and the contractional tectonic transport vector, and their spatial position. The study of flexural normal faults is a powerful tool for collecting information about the age of the fold-and-thrust belt and the foredeep flexure, the trend of the fold-and-thrust belt front, the type of thrust propagation sequence, the degree of tightening of the foredeep flexure, rates of deformation propagation across and along strike, and the variation of these parameters both across and along strike. In order to obtain these results, a set of very simple techniques has been designed based on the analysis of syn-extensional beds related to the normal faults or dated normal faults, the strike of the normal faults, temporal relationships between normal faults and thrusts and folds, fracturing intensity measurements, and distance between dated normal faults measured both across and along strike.

Our approach has been applied to a natural fold-and-thrust belt to ascertain some of the issues mentioned above. The belt chosen is the Cantabrian Zone, which is the foreland fold-and-thrust belt of the Variscan orogen in the NW portion of the Iberian Peninsula, located in the core of the Ibero-Armorican or Asturian Arc. The pre-folding and pre-thrusting normal faults mapped in various Cantabrian-Zone thrust sheets have been interpreted here as flexural normal faults linked to foredeep flexures caused in intermediate stages of emplacement of the fold-and-thrust belt. These flexures have not been preserved due to overprinting by later folds and thrusts. The trend of the old orogenic front deduced from the strike of the longitudinal flexural normal faults exhibits an arc-shaped arrangement, consistent with the geometry of the Ibero-Armorican or Asturian Arc. The results obtained indicate that the orogenic front was more linear in the Arc southern branch than in the northern one, and that the front was more advanced towards the foreland in the northern branch. The relative temporal relationship between the flexural normal faults and contractional structures indicates that the thrust propagation sequence was a forward-breaking or “piggy-back” sequence. This result agrees with the thrust propagation sequence deduced in the literature using other techniques. The low areal intensity of fracturing due to longitudinal flexural normal faults suggests that the flexure curvature and the dip of the flexure inclined limb were very gentle, while the flexure interlimb angle was very high. This might indicate that the fold-and-thrust belt weight at the time of formation of these normal faults was low. The transverse flexural normal faults, found in the southwestern part of the Cantabrian Zone, have been correlated with a lateral and an oblique thrust ramp. This points out that the tectonic load due to the fold-and-thrust belt advance was variable along strike.

All the criteria and methodology presented in this study, and applied to the Cantabrian Zone foreland fold-and-thrust belt, can be applied in similar settings.

Care must be taken when performing outcrop-scale restorations of fold/thrust structures in fold-and-thrust belts developed according to a forward-breaking thrust propagation sequence. In these regions, layer-cake stratigraphy may not be always the best template, as beds may be cut and offset by flexural normal faults developed prior to the contractional structures. This could introduce anomalies in the restored sections, which should not be attributed to the section viability. Rather, these anomalies may result from the original layers attitude.

CRediT authorship contribution statement

Mayte Bulnes: Writing – review & editing, Visualization, Validation, Supervision, Resources, Project administration, Methodology, Investigation, Formal analysis, Conceptualization. **Hodei Uzkeda:** Writing – review & editing, Visualization, Validation, Supervision, Resources, Project administration, Methodology, Investigation, Formal analysis, Conceptualization. **Josep Poblet:** Writing – review & editing, Writing – original draft, Visualization, Validation, Resources, Project administration, Methodology, Investigation, Funding acquisition, Formal analysis, Conceptualization. **Iván García Zuazua:** Resources, Methodology, Investigation, Formal analysis.

Declaration of competing interest

The authors declare that they have no known competing financial interests or personal relationships that could have appeared to influence the work reported in this paper.

Acknowledgments

Richard Lisle carried out a stay at the University of Oviedo, which allowed us to learn a great deal from him and get to know him as a person. We hope this contribution is a worthy tribute to Richard, an excellent structural geologist, a great professor, and an outstanding person. We deeply regret his loss. We thank Fernando Bastida, whose effort and dedication brought Richard to Oviedo. We appreciate the comments and suggestions from reviewers Paolo Pace and Gabriel Gutiérrez-Alonso, and from Guest Editor Enrico Tavarnelli, which have contributed to improve the manuscript. We would also like to thank Enrico Tavarnelli, Tom Blenkinsop, Julia Gale and Ian Alsop for editing this special volume "From Folds to Faults" in honour of Richard. Finally, we acknowledge financial support from the research project PID2021-126357NB-100, funded by the Spanish Ministry of Science and Innovation.

Data availability

All data used in this study are contained within this article.

References

Adrichem Boogaert, van, H.A., 1965. Conodont-bearing formations of Devonian and Lower Carboniferous age in the northern León and Palencia (Spain). Leidse Geologische Mededelingen 31, 165–178.
Aller, J., Álvarez-Marrón, J., Bastida, F., Bulnes, M., Heredia, N., Marcos, A., Pérez-Estaún, A., Pulgar, J.A., Rodríguez-Fernández, R., 2004. Estructura, deformación y metamorfismo (Zona Cantábrica). In: Vera, J.A. (Ed.), Geología De España. Sociedad Geológica de España-Instituto Geológico y Minero de España, Madrid, pp. 42–49.
Allmendinger, R.W., Cardozo, N.C., Fisher, D., 2013. Structural Geology Algorithms: Vectors & Tensors. Cambridge University Press, Cambridge, p. 289.
Almela, A., García Fuente, S., Ríos, J.M., 1956. Mapa Geológico de España. Escala 1: 50.000. Hoja 52: Proaza. Instituto Geológico y Minero de España, Madrid.
Alonso, J.L., 1987. Estructura y evolución tectonoestratigráfica de la Región del Manto del Esla (Zona Cantábrica, NW de España). Institución Fray Bernardino De Sahagún, Diputación Provincial De León.
Alonso, J.L., Álvarez-Marrón, J., Pulgar, J.A., 1989. Síntesis cartográfica de la parte sudoccidental de la Zona Cantábrica. Trab. Geol. 18, 145–155.
Alonso, J.L., Álvarez-Marrón, J., Aller, J., Bastida, F., Farias, P., Marcos, A., Marquínez, J., Pérez-Estaún, A., Pulgar, J.A., 1992. Estructura de la Zona Cantábrica. In: Liso Rubio, M.J., Gutiérrez Marco, J.C., Saavedra Alonso, J., Rábano Gutiérrez del Arroyo, I. (Eds.), Paleozoico Inferior De Ibero-América. Universidad de Extremadura, Badajoz, pp. 423–434.
Alonso, J.L., Pulgar, J.A., García-Ramos, J.C., Barba, P., 1996. Tertiary basins and Alpine tectonics in the Cantabrian Mountains (NW Spain). In: Friend, P.F., Dabrio, C.J. (Eds.), Tertiary Basins of Spain: the Stratigraphic Record of Crustal Kinematics. Cambridge University Press, Cambridge, pp. 214–227.
Alonso, J.L., Gallastegui, J., Garcia-Ramos, J.C., Poblet, J., 2009a. Estructuras mesozoicas y cenozoicas relacionadas con la apertura y cierre parcial del Golfo de Vizcaya (Zona Cantábrica – Asturias). Guía De Campo Del "6° Simposio Sobre El Margen Ibérico Atlántico", p. 18. Oviedo.
Alonso, J.L., Marcos, A., Suárez, A., 2009b. Paleogeographic inversion resulting from large out of sequence breaching thrusts: the León Fault (Cantabrian Zone, NW Iberia). A new picture of the external Variscan Thrust Belt in the Ibero-Armorican Arc. Geol. Acta 7 (4), 451–473.
Alonso, J.L., Colombo, F., Riba, O., 2011. Folding mechanisms in a fault-propagation fold inferred from the analysis of unconformity angles: the Sant Llorenç growth structure (Pyrenees, Spain). In: McClay, K., Shaw, J., Suppe, J. (Eds.), Thrust fault-related Folding, 94. AAPG Memoir, pp. 137–151.
Alonso, J.L., Barrón, E., González Fernández, B., Menéndez Casares, E., García-Ramos, J. C., 2016. Extensión e inversión tectónica alpinas en el área de Sariego. Control ejercido por la estructura varisca subyacente (Asturias, norte de España). Trab. Geol. 35, 45–60.
Alonso López, M., 2014. Análisis estructural de los materiales Jurásicos de la playa de El Rinconín, Gijón. Universidad de Oviedo, p. 47. MSc Thesis.
Álvarez-Marrón, J., Hetzel, R., Niedermann, S., Menéndez, R., Marquínez, J., 2008. Origin, structure and exposure history of a wave-cut platform more than 1 Ma in age at the coast of northern Spain: a multiple cosmogenic nuclide approach. Geomorphology 93 (3–4), 316–334.
American Society for Testing and Materials, 2001. Standard test method for determination of rock hardness by rebound hammer method. ASTM Stand, 04.09 (D 5873-00).
Aydin, A., Basu, A., 2005. The Schmidt hammer in rock material characterization. Eng. Geol. 81 (1), 1–14.
Barrois, C.E., 1882. Recherches sur le terrains anciens des Asturies et de la Galice. Memoires de la Societé Géologique du Nord 2 (1), 1–630.
Bastida, F., Gutiérrez, G., 1989. Síntesis cartográfica de las unidades occidentales de la Zona Cantábrica (NO de España). Trab. Geol. 18, 117–125.
Bastida, F., Marcos, A., Pérez-Estaún, A., Pulgar, J.A., 1984. Geometría y evolución estructural de la lámina cabalgante de Somiedo (Zona Cantábrica, NO de España). Boletín del Instituto Geológico y Minero de España 95 (6), 517–539.
Beaumont, C., 1981. Foreland basins. Geophys. J. Int. 65 (2), 291–329.
Boyer, S.E., 1986. Styles of folding within thrust sheets: examples from the Appalachian and Rocky Mountains of the USA and Canada. J. Struct. Geol. 8 (3–4), 325–339.
Bradley, D.C., Kidd, W.S.F., 1991. Flexural extension of the upper continental crust in collisional foredeeps. GSA Bulletin 103 (11), 1416–1438.
Bulnes, M., 1989. La Estructura Del Área situada en el entorno de las localidades de Trubia, Proaza y Sama de Grado (Zona Cantábrica, NO de España). Seminario de Investigación. Universidad de Oviedo, p. 23.
Bulnes, M., 1995. La estructura geológica del Valle del Trubia (Zona Cantábrica, NO de España). PhD thesis. Universidad de Oviedo, p. 255.
Bulnes, M., Aller, J., 2002. Three-dimensional geometry of large-scale fault-propagation folds in the Cantabrian Zone, NW Iberian Peninsula. J. Struct. Geol. 24 (4), 827–846.
Bulnes, M., Marcos, A., 2001. Internal structure and kinematics of Variscan thrust sheets in the valley of the Trubia River (Cantabrian Zone, NW Spain): regional tectonic implications. Int. J. Earth Sci. 90, 287–303.
Bulnes, M., García-Alcalde, J.L., Marcos, A., 1999. Litoestratigrafía del Grupo Rañeces (Devónico inferior) en el Antiforme de Caranga-Trubia (Zona Cantábrica, NO de España). Rev. Soc. Geol. Espana 12 (3), 339–349.
Bulnes, M., Poblet, J., de Ana, Á., Masini, M., 2016. Comportamiento de las calizas «griotte» carboníferas frente a deformaciones compresivas en dos localidades de la Zona Cantábrica (NO de la Península Ibérica): resultados preliminares. Trab. Geol. 36, 61–80.
Bulnes, M., Poblet, J., Uzkeda, H., Rodriguez-Alvarez, I., 2019. Mechanical stratigraphy influence on fault-related folds development: insights from the Cantabrian Zone (NW Iberian Peninsula). J. Struct. Geol. 118, 87–103.
Butler, R.W.H., 1987. Thrust sequences. J. Geol. Soc. 144 (4), 619–634.
Cadenas, P., Fernández-Viejo, G., 2017. The Asturian Basin within the North Iberian margin (Bay of Biscay): seismic characterisation of its geometry and its Mesozoic and Cenozoic cover. Basin Res. 29, 521–541.
Calamita, F., Di Domenica, A., Pace, P., 2018. Macro-and meso-scale structural criteria for identifying pre-thrusting normal faults within foreland fold-and-thrust belts: insights from the Central-Northern Apennines (Italy). Terra Nova 30 (1), 50–62.
Caldera Grau, N., 2016. Geometría, cinemática y rocas de falla en la parte basal del Manto de Somiedo (Región de Babia, Noroeste de España). Universidad de Oviedo, p. 47. MSc thesis.
Chester, J.S., Logan, J.M., Spang, J.H., 1991. Influence of layering and boundary conditions on fault-bend and fault-propagation folding. GSA Bulletin 103 (8), 1059–1072.
Chou, Y.-W., Yu, H.-S., 2002. Structural expressions of flexural extension in the arc-continent collisional foredeep of western Taiwan. In: Byrne, T.,B., Liu, C.S. (Eds.), Geology and Geophysics of an arc-continent Collision, 358. GSA Special Paper, Taiwan, pp. 1–12.
Cloos, E., 1968. Experimental analysis of Gulf Coast fracture patterns. AAPG (Am. Assoc. Pet. Geol.) Bull. 52 (3), 420–444.
Cobbold, P.R., Szatmari, P., Demercian, L.S., Coelho, D., Rossello, E.A., 1995. Seismic and experimental evidence for thin-skinned horizontal shortening by convergent radial gliding on evaporites, deep-water Santos Basin, Brazil. In: Jackson, M.P.A., Roberts, D.G., Snelson, S. (Eds.), Salt Tectonics: a Global Perspective, 65. AAPG Memoir, pp. 305–321.
Davison, I., 1986. Listric normal fault profiles: calculation using bed-length balance and fault displacement. J. Struct. Geol. 8, 209–210.
Davison, I., Alsop, I., Birch, P., Elders, C., Evans, N., Nicholson, H., Rorison, P., Wade, D., Woodward, J., Young, M., 2000. Geometry and late-stage structural evolution of Central Graben salt diapirs, North Sea. Mar. Petrol. Geol. 17 (4), 499–522.
de Oliveira Neto, E.R., Fernandes, F.J.D., Fatah, T.Y.A., Dias, R.M., da Piedade, Z.R.T., Freire, A.F.M., Lupinacci, W.M., 2025. A data-driven approach to predict fracture intensity using machine learning for presalt carbonate reservoirs: a feasibility study in the Mero Field, Santos Basin, Brazil. Energy Geoscience, 100404.
De Paz Álvarez, M.I., 2023. Deformación y rocas de falla en las zonas de cizalla basales de los mantos cantábricos. PhD thesis. Universidad de Oviedo, p. 525.
De Sitter, L.U., Van den Bosch, W.J., 1969. The structure of the SW part of the Cantabrian Mountains. Leidse Geol. Meded. 43 (1), 213–215.
DeCelles, P.G., 2011. Foreland basin systems revisited: variations in response to tectonic settings. In: Busby, C., Azor, A. (Eds.), Tectonics of Sedimentary Basins: Recent Advances. Blackwell Publishing Ltd., Chichester, pp. 405–426.
DeCelles, G., Giles, K.N., 1996. Foreland basin systems. Basin Res. 8, 105–123.
Doglioni, C., 1993. Some remarks on the origin of foredeeps. Tectonophysics 228 (1–2), 1–20.
Doglioni, C., 1995. Geological remarks on the relationships between extension and convergent geodynamic settings. Tectonophysics 252 (1–4), 253–267.
Dreyfuss, M., Grandjacquet, C., Chauvé, P., Dudan, R., Chauve, M., Bulle, J., Both, J., Colas, G., Cassedanne, J., Sainton, C., Ziegler, M., 1968. Carte de France au 50.000^{e} (type 1922) Ornans. Bureau de Recherches Géologiques et MInières, Orléans.
Elliott, D., 1976. The energy balance and deformation mechanisms of thrust sheets. Phil. Trans. Roy. Soc. Lond. 283, 289–312.
Epard, J.L., Groshong Jr, R.H., 1995. Kinematic model of detachment folding including limb rotation, fixed hinges and layer-parallel strain. Tectonophysics 247 (1–4), 85–103.
Fernández-López, S., Suárez Vega, L.C., 1981. Estudio bioestratigráfico (Ammonoidea) del Aaleniense y Bajociense en Asturias. Estud. Geol. 35 (1–6), 231–239.
Fiore Allwardt, P., Bellahsen, N., Pollard, D.D., 2007. Curvature and fracturing based on global positioning system data collected at Sheep Mountain anticline, Wyoming. Geosphere 3 (6), 408–421.

Flemings, B., Jordan, T.E., 1989. A synthetic stratigraphic model of foreland basin development. J. Geophys. Res. 94, 3851–3866.
Flor, G., 1983. Las rasas asturianas: ensayos de correlación y emplazamiento. Trab. Geol. 13, 65–83.
Freund, R., 1971. The Hope Fault: a strike-slip fault in New Zealand. New Zealand Geological Survey Bulletin 86, 1–49.
García Fuente, S., 1952. Geología del Concejo de Teverga (Asturias), 64. Boletín del Instituto Geológico y Minero de España, pp. 345–456.
García Fuente, S., 1953. Geología de los Concejos de Proaza y Tameza (Asturias), 65. Boletín del Instituto Geológico y Minero de España, pp. 271–324.
Geiser, J., Geiser, P.A., Kligfield, R., Ratliff, F., Rowan, M., 1988. New applications of computer-based section construction: strain analysis, local balancing and subsurface fault prediction. Mount. Geol. 25 (2), 47–59.
Gray, D.R., 1981. Cleavage-fold relationships and their implications for transected folds: an example from southwest Virginia, USA. J. Struct. Geol. 3 (3), 265–277.
Groshong Jr, R.H., 1989. Half-graben structures: balanced models of extensional fault-bend folds. GSA Bulletin 101 (1), 96–105.
Gutiérrez Alonso, G., 1992. El Antiforme del Narcea y su relación con los mantos occidentales de la Zona Cantábrica. Universidad de Oviedo. PhD thesis.
Gutiérrez Claverol, M., Fernández, C.L., Alonso, J.L., 2006. Procesos neotectónicos en los depósitos de rasa de la zona de Canero (Occidente de Asturias). Geogaceta 40, 75–78.
Hardy, S., Poblet, J., 1994. Geometric and numerical model of progressive limb rotation in detachment folds. Geology 22 (4), 371–374.
Heredia, N., 1984. La estructura de la escama de Villar de Vildas (Manto de Somiedo, Zona Cantábrica). Trab. Geol. 14, 65–79.
Instituto Geológico y Minero de España, 2021. Geode. Mapa Geológico Continuo de España a escala 1/50.000. https://info.igme.es/cartografiadigital/geologica/geode.aspx. (Accessed 9 January 2025).
Julivert, M., 1971. Décollement tectonics in the Hercynian Cordillera of NW Spain. Am. J. Sci. 270, 1–29.
Julivert, M., 1979. A cross-section through the northern part of the Iberian Massif: its position within the Hercynian fold belt. Krystalinikum 14, 51–67.
Julivert, M., 1981. Cross-section through the northern part of the Iberian Massif. Geologie en Minbouw 60, 107–128.
Julivert, M., 1983. La estructura de la Zona Cantábrica. In: Comba, J.A. (Ed.), Geología de España. Libro Jubilar. Instituto Geológico y Minero de España, Madrid, pp. 339–381. J. M. Ríos, Tomo I.
Julivert, M., Arboleya, M.L., 1984. Curvature increase and structural evolution of the core (Cantabrian Zone) of the Ibero-Armorican Arc. Sciences Géologiques, bulletins et mémoires 37 (1), 5–11.
Julivert, M., Marcos, A., 1973. Superimposed folding under flexural conditions in the Cantabrian Zone (Hercynian Cordillera, northwest Spain). Am. J. Sci. 273 (5), 353–375.
Julivert, M., Pello, J., Fernández-García, L., 1968. La estructura del manto de Somiedo (Cordillera Cantábrica). Trab. Geol. 2, 1–45.
Julivert, M., del Pozo, J.R., Truyols, J., 1971. Le réseau de failles et la couverture Post-hercynienne dans les Asturies. Editions Technip, Paris.
Julivert, M., Fontboté, J.M., Ribeiro, A., Conde, L.E., 1972. Mapa Tectónico de la Península Ibérica y Baleares, E. 1:1000000. Instituto Geológico y Minero de España, Madrid.
Khalil, S.M., McClay, K.R., 2002. Extensional fault-related folding, northwestern Red Sea, Egypt. J. Struct. Geol. 24 (4), 743–762.
Lacombe, O., Beaudoin, N.E., 2024. Timing, sequence, duration and rate of deformation in fold-and-thrust belts: a review of traditional approaches and recent advances from absolute dating (K–Ar illite/U–Pb calcite) of brittle structures. C. R. Geosci. 356 (S2), 467–494.
Lepvrier, C., Martínez-García, E., 1990. Fault development and stress evolution of the post-Hercynian Asturian Basin (Asturias and Cantabria, northwestern Spain). Tectonophysics 184 (3–4), 345–356.
Leyva, F., Matas, J., Rodríguez-Fernández, L.R., García Alcalde, J., Arbizu, M., García López, S., Arias, L., 1984. Memoria del Mapa Geológico de España. Escala 1:50.000. Hoja 129: La Robla. Instituto Geológico y Minero de España, Madrid, p. 98.
Lisle, R.J., 1994. Detection of zones of abnormal strains in structures using Gaussian curvature analysis. AAPG (Am. Assoc. Pet. Geol.) Bull. 78 (12), 1811–1819.
López-Fernández, C., Pulgar, J.A., Gallart, J., González-Cortina, J.M., Díaz, J., Ruiz, M., 2004. Actividad sísmica en el noroeste de la Península Ibérica observada por la red sísmica local del Proyecto GASPI, 1999-2002. Trab. Geol. 24, 91–107.
López-Gómez, J., Martín-González, F., Heredia, N., de la Horra, R., Barrenechea, J.F., Cadenas, P., Juncal, M., Diez, J.B., Borruel-Abadía, V., Pedreira, D., García-Sansegundo, J., Farias, P., Galé, C., Lago, M., Ubide, T., Fernández-Viejo, G., Gand, G., 2019. New lithostratigraphy for the Cantabrian Mountains: a common tectono-stratigraphic evolution for the onset of the Alpine cycle in the W pyrenean realm, N Spain. Earth Sci. Rev. 188, 249–271.
Lotze, F., 1945. Zur gliederung der varisziden der Iberischen Meseta. Geotekt. Forsch. 6, 78–92.
Magán, M., 2017. Análisis de la fracturación en un anticlinal desarrollado en rocas jurásicas en la playa Peñarrubia, Gijón (Cuenca Asturiana, NO de la Península Ibérica). Universidad de Oviedo, p. 62. MSc thesis.
Magán, M., 2024. Desarrollo de una base de datos y herramientas para el análisis estructural de datos de campo y de modelos de afloramientos virtuales: Aplicación a rocas jurásicas deformadas de la costa de Gijón (Cuenca Asturiana, N de la Península Ibérica). PhD thesis. Universidad de Oviedo, p. 267.
Magán, M., Poblet, J., Bulnes, M., 2022. Tools to analyse misleading kinematic interpretations of faults offsetting inclined or folded surfaces: applications to Asturian Basin (NW Iberian Peninsula) examples. J. Struct. Geol. 162, 104687.
Martínez-Álvarez, J.A., Gutiérrez Claverol, M., Torres-Alonso, M., 1975. Memoria del Mapa Geológico de España. Escala 1:50.000. Hoja 28: Grado. Instituto Geológico y Minero de España, Madrid, p. 49.
Mary, G., 1983. Evolución del margen costero de la Cordillera Cantábrica en Asturias desde el Mioceno. Trab. Geol. 13, 3–37.
Masaferro, J.L., Bulnes, M., Poblet, J., Casson, N., 2003. Kinematic evolution and fracture prediction of the Valle Morado structure inferred from 3-D seismic data, Salta province, northwest Argentina. AAPG (Am. Assoc. Pet. Geol.) Bull. 87 (7), 1083–1104.
Masini, M., Bulnes, M., Poblet, J., 2010a. Cross-section restoration: a tool to simulate deformation. Application to a fault-propagation fold from the Cantabrian fold and thrust belt, NW Iberian Peninsula. J. Struct. Geol. 32, 172–183.
Masini, M., Poblet, J., Bulnes, M., 2010b. Structural analysis and deformation architecture of a fault-propagation fold in the southern Cantabrian Mountains, NW Iberian Peninsula. Trab. Geol. 30, 55–62.
Masini, M., Bigi, S., Poblet, J., Bulnes, M., Di Cuia, R., Casabianca, D., 2011. Kinematic evolution and strain simulation, based on cross section restoration, of the Maiella Mountain: an analogue for oil fields in the Apennines (Italy). In: Poblet, J., Lisle, R. (Eds.), Kinematic Evolution and Structural Styles of fold-and-thrust Belts, 349. Geological Society Special Publication, pp. 25–44.
Mauldon, M., Dunne, W.M., Rohrbaugh Jr, M.B., 2001. Circular scanlines and circular windows: new tools for characterizing the geometry of fracture traces. J. Struct. Geol. 23 (2–3), 247–258.
McClay, K.R., 1990. Extensional fault systems in sedimentary basins: a review of analogue model studies. Mar. Petrol. Geol. 7 (3), 206–233.
McClay, K.R., 1992. Glossary of thrust tectonics terms. In: McClay, K.R. (Ed.), Thrust Tectonics. Chapman & Hall, London, pp. 419–433.
McClay, K.R., 1996. Recent advances in analogue modelling: uses in section interpretation and validation. In: Buchanan, E.G., Nieuwland, D.A. (Eds.), Modem Developments in Structural Interpretation, Validation and Modelling, 99. Geological Society Special Publication, pp. 201–225.
McClay, K., Dooley, T., 1995. Analogue models of pull-apart basins. Geology 23 (8), 711–714.
McNeill, L.C., Piper, K.A., Goldfinger, C., Kulm, L.D., Yeats, R.S., 1997. Listric normal faulting on the Cascadia continental margin. J. Geophys. Res. Solid Earth 102 (B6), 12123–12138.
Méndez-Bedia, I., 1976. Biofacies y litofacies de la formación Moniello-Santa Lucía (Devónico de la Cordillera Cantábrica, NW de España). Trab. Geol. 9, 3–93.
Merino-Tomé, O., Gutiérrez-Alonso, G., Villa, E., Fernández-Suárez, J., Llaneza, J.M., Hofmann, M., 2017. LA-ICP-MS U-Pb dating of Carboniferous ash layers in the Cantabrian Zone (N Spain): stratigraphic implications. J. Geol. Soc. 174 (5), 836–849.
Mitra, S., Paul, D., 2011. Structural geometry and evolution of releasing and restraining bends: insights from laser-scanned experimental models. AAPG (Am. Assoc. Pet. Geol.) Bull. 95 (7), 1147–1180.
Moretti, I., Colletta, B., Vially, R., 1988. Theoretical model of block rotation along circular faults. Tectonophysics 153, 313–320.
Muñoz, J.A., McClay, K., Poblet, J., 1994. Synchronous extension and contraction in frontal thrust sheets of the Spanish Pyrenees. Geology 22 (10), 921–924.
Navarro Vázquez, D., Rodríguez-Fernández, L.R., 1982. Mapa geológico de España. Escala 1:50.000. Hoja 101: Villablino. Instituto Geológico y Minero de España, Madrid.
Odriozola, M., 2016. Extensión y compresión en los materiales jurásicos de la playa de Peñarrubia. Universidad de Oviedo, Gijón, p. 31. MSc Thesis.
Pace, P., Pasqui, V., Tavarnelli, E., Calamita, F., 2017. Foreland-directed gravitational collapse along curved thrust fronts: insights from a minor thrust-related shear zone in the Umbria–Marche belt, central-northern Italy. Geol. Mag. 154 (2), 381–392.
Pello Muñiz, J., 1974. Mapa Geológico de España. Escala 1:50.000. Hoja 52: Proaza. Instituto Geológico y Minero de España, Madrid.
Pello Muñíz, J., Martínez Díaz, C., Leyva, F., Fernández Luanco, M.C., del Pan, T., 1976. Memoria del Mapa Geológico de España. Escala 1:50.000. Hoja 52: Proaza. Instituto Geológico y Minero de España, Madrid, p. 53.
Pérez-Estaún, A., Bastida, F., 1990. Cantabrian Zone: structure. In: Dallmeyer, R.D., Martínez-García, E. (Eds.), Pre-Mesozoic Geology of Iberia. Springer-Verlag, Berlin, pp. 55–69.
Pérez-Estaún, A., Bastida, F., Alonso, J.L., Marquínez, J., Álvarez-Marrón, J., Marcos, A., Pulgar, J.A., 1988. A thin-skinned tectonics model for an arcuate fold and thrust belt: the Cantabrian Zone (Variscan Ibero-Armorican Arc). Tectonics 7, 517–537.
Poblet, J., 2020. Cartographic pattern of terminations of simple, parallel fault-bend folds, fault-propagation folds and detachment folds. J. Struct. Geol. 138, 104135.
Poblet, J., Bulnes, M., 2005. Fault-slip, bed-length and area variations in experimental rollover anticlines over listric normal faults: influence in extension and depth to detachment estimations. Tectonophysics 396, 97–117.
Poblet, J., Lisle, R., 2011. Kinematic evolution and structural styles of fold-and-thrust belts. In: Poblet, J., Lisle, R. (Eds.), Kinematic Evolution and Structural Styles of fold-and-thrust Belts, 349. Geological Society Special Publication, pp. 1–24.
Poblet, J., McClay, K., 1996. Geometry and kinematics of single-layer detachment folds. AAPG (Am. Assoc. Pet. Geol.) Bull. 80 (7), 1085–1109.
Poblet, J., McClay, K., Storti, F., Muñoz, J.A., 1997. Geometries of syntectonic sediments associated with single-layer detachment folds. J. Struct. Geol. 19 (3–4), 369–381.
Poblet, J., Muñoz, J.A., Travé, A., Serra-Kiel, J., 1998. Quantifying the kinematics of detachment folds using three-dimensional geometry: application to the Mediano anticline (Pyrenees, Spain). GSA Bulletin 110 (1), 111–125.
Poblet, J., Bulnes, M., Uzkeda, H., Magán, M., 2022. Using the Schmidt hammer on folds: an example from the Cantabrian Zone (NW Iberian Peninsula). J. Struct. Geol. 155, 104512.

Proceq, 2016. Rock Schmidt. Operating Instructions. Proceq S.A., Schwerzenbach.
Pulgar, J.A., Alonso, J.L., Espina, R.G., Marín, J.A., 1999. La deformación alpina en el basamento varisco de la Zona Cantábrica. Trab. Geol. 21, 283–294.
Ramsay, J.G., 1967. Folding and Fracturing of Rocks. McGraw Hill Book Company, USA, p. 568.
Ramsay, J.G., Huber, M.I., 1987. The techniques of modern structural geology. In: Folds and Fractures, 2. Academic press, London, p. 700.
Rodríguez, I., 2020. Estructura de la parte sumergida del Cinturón de Sinú y de la parte adyacente de la Cuenca de Colombia (Margen Caribeño al NO de Colombia). Universidad de Oviedo, p. 183. PhD thesis.
Rodríguez, I., Bulnes, M., Poblet, J., Masini, M., Flinch, J., 2021. Structural style and evolution of the offshore portion of the Sinu Fold Belt (south Caribbean Deformed Belt) and adjacent part of the Colombian Basin. Mar. Petrol. Geol. 125, 104862.
Rodríguez, I., Poblet, J., Bulnes, M., Flinch, J., Masini, M., 2022a. Horizontal/vertical motion and wedge geometry of the Sinú Fold Belt, south-caribbean accretionary prism, NW Colombia: implications for a morphostructural zoning. Mar. Petrol. Geol. 143, 105780.
Rodríguez, I., Poblet, J., Bulnes, M., Masini, M., Flinch, J., 2022b. Thrust sequence in the Sinú Fold Belt (south Caribbean Deformed Belt), offshore northwestern Colombia. In: Zamora, G., Mora, A. (Eds.), Andean Structural Styles. A Seismic Atlas. Elsevier, Amsterdam, pp. 111–119.
Rodríguez, I., Bulnes, M., Poblet, J., Flinch, J., Masini, M., 2022c. Relationships between normal faulting, mud diapirism and thrusting in the trailing part of the Sinú Fold Belt (south Caribbean Deformed Belt), offshore northwestern Colombia. In: Zamora, G., Mora, A. (Eds.), Andean Structural Styles. A Seismic Atlas. Elsevier, Amsterdam, pp. 121–128.
Rodríguez-Fernández, L.R., Navarro Vázquez, D., Laboratorios de ENADIMSA, Departamento de Paleontología de la Universidad de Oviedo, 1982. Memoria Del Mapa Geológico De España. Escala 1:50.000. Hoja 101: Villablino. Instituto Geológico y Minero de España, Madrid, p. 56.
Rodríguez-Fernández, L.R., Barba, P., Fernández, L.P., Bardají, T., Silva, P.G., Suárez-Rodríguez, A., Heredia, N., Gallastegui, G., Paniagua, A., Galán, L., Martínez Álvarez, J.A., Torres Alonso, M., Gutiérrez Claverol, M., López Díaz, F., Toyos, J.M., Villa, E., Salvador González, C., Bravo Fernández, I., 1991. Memoria Del Mapa Geológico De España. Escala 1:50.000. Hoja 102: Los Barrios De Luna. Instituto Tecnológico y Geominero de España, Madrid, p. 130.
Rohrbaugh, Jr, M.B., Dunne, W.M., Mauldon, M., 2002. Estimating fracture trace intensity, density, and mean length using circular scan lines and windows. AAPG (Am. Assoc. Pet. Geol.) Bull. 86 (12), 2089–2104.
Salvini, F., Storti, F., 2004. Active-hinge-folding-related deformation and its role in hydrocarbon exploration and development insights from HCA modeling. In: McClay, K.R. (Ed.), Thrust Tectonics and Hydrocarbon Systems, 82. AAPG Memoir, pp. 453–472.
Savage, J.F., 1979. The Hercynian orogeny in the Cantabrian mountains, Northern Spain. Krystalinikum 14, 91–108.
Savage, J.F., 1981. Geotectonic cross-section through the Cantabrian mountains, northern Spain. Geol. Mijnbouw 81, 3–5.
Scisciani, V., 2009. Styles of positive inversion tectonics in the Central Apennines and in the Adriatic foreland: implications for the evolution of the Apennine chain (Italy). J. Struct. Geol. 31 (11), 1276–1294.
Scisciani, V., Calamita, F., Tavarnelli, E., Rusciadelli, G., Ori, G.G., Paltrinieri, W., 2001. Foreland-dipping normal faults in the inner edges of syn-orogenic basins: a case from the Central Apennines, Italy. Tectonophysics 330 (3–4), 211–224.
Scisciani, V., Tavarnelli, E., Calamita, F., Paltrinieri, W., 2002. Pre-thrusting normal faults within syn-orogenic basins of the Outer Central Apennines, Italy: implications for apennine tectonics. Bolletino Societa Geologica Italiana, Special Volume 1, 295–304.
Sharp, I.R., Gawthorpe, R.L., Underhill, J.R., Gupta, S., 2000. Fault-propagation folding in extensional settings: examples of structural style and synrift sedimentary response from the Suez rift, Sinai, Egypt. GSA Bulletin 112 (12), 1877–1899.
Smith, M., Chantraprasert, S., Morley, C.K., Cartwright, I., 2007. Structural geometry and timing of deformation in the Chainat duplex, Thailand. In: Cunningham, W.D., Mann, P. (Eds.), Tectonics of strike-slip Restraining and Releasing Bends, 290. Geological Society Special Publication, pp. 305–323.
Soleimany, B., Poblet, J., Bulnes, M., Sàbat, F., 2011. Fold amplification history unravelled from growth strata: the Dorood anticline, NW Persian Gulf. J. Geol. Soc. 168 (1), 219–234.
Suárez-Rodríguez, Á., 1988. Estructura del área de Villaviciosa-Libardón (Asturias, Cordillera Cantábrica). Trab. Geol. 17, 87–98.
Suárez-Rodríguez, A., Toyos, J.M., López Díaz, F., Heredia, N., Rodríguez-Fernández, L. R., Gutiérrez-Alonso, G., 1988-89. Mapa Geológico De España. Escala 1:50.000. Hoja 102: Los Barrios De Luna. Instituto Tecnológico y Geominero de España, Madrid.
Suess, E., 1892. Das Antlitz Der Erde. F. Tempsky, Wien.
Suppe, J., 1983. Geometry and kinematics of fault-bend folding. Am. J. Sci. 283 (7), 684–721.
Suppe, J., Medwedeff, D.A., 1990. Geometry and kinematics of fault-propagation folding. Eclogae Geol. Helv. 83 (3), 409–454.
Uzkeda, H., 2013. Reconstrucción 3D Y análisis estructural de las rocas Jurásicas de Colunga-Tazones (Cuenca Asturiana, NO De La Península Ibérica). Universidad de Oviedo, p. 259. PhD thesis.
Uzkeda, H., Bulnes, M., Poblet, J., García-Ramos, J.C., Piñuela, L., 2013. Buttressing and reverse reactivation of a normal fault in the Jurassic rocks of the Asturian Basin, NW Iberian Peninsula. Tectonophysics 599, 117–134.
Uzkeda, H., Bulnes, M., Poblet, J., García-Ramos, J.C., Piñuela, L., 2016. Jurassic extension and Cenozoic inversion tectonics in the Asturian Basin, NW Iberian Peninsula: 3D structural model and kinematic evolution. J. Struct. Geol. 90, 157–176.
Uzkeda, H., Poblet, J., Bulnes, M., Martín, S., 2018. Effects of inherited structures on inversion tectonics: examples from the Asturian Basin (NW Iberian Peninsula) interpreted in a Computer Assisted Virtual Environment (CAVE). Geosphere 14 (4), 1635–1656.
Uzkeda, H., Poblet, J., Magán, M., Bulnes, M., Martín, S., Fernández-Martínez, D., 2022. Virtual outcrop models: Digital techniques and an inventory of structural models from North-Northwest Iberia (Cantabrian Zone and Asturian Basin). J. Struct. Geol. 157, 104568.
Uzkeda, H., Poblet, J., Bulnes, M., 2025. Late Triassic to present-day tectono-thermal history of the coastal part of the Asturian basin: implications for hydrocarbon exploration and for the North-Iberian margin evolution. Mar. Petrol. Geol. 171, 107158.
Valenzuela, M., García-Ramos, J.C., Suárez de Centi, C., 1986. The Jurassic sedimentation in Asturias (N Spain). Trab. Geol. 16, 121–132.
Valenzuela, M., García-Ramos, J.C., Suárez de Centi, C., 1989. La sedimentación en una rampa carbonatada dominada por tempestades, ensayos de correlación de ciclos y eventos en la ritmita margo-calcárea del Jurásico de Asturias. Cuad. Geol. Iber. 13, 217–235.
Valero, L., Soleimany, B., Bulnes, M., Poblet, J., 2015. Evolution of the Nourooz anticline (NW Persian Gulf) deciphered using growth strata: structural inferences to constrain hydrocarbon exploration in Persian offshore anticlines. Mar. Petrol. Geol. 66, 873–889.
Van den Bosch, W.J., 1969. Geology of the Luna-Sil region, cantabrian Mountains (NW Spain). Leidse Geol. Meded. 44 (1), 137–225.
Van der Voo, R., Stamatakos, J.A., Parés, J.M., 1997. Kinematic constraints on thrust-belt curvature from syndeformational magnetizations in the Lagos del Valle syncline in the Cantabrian Arc, Spain. J. Geophys. Res. Solid Earth 102 (B5), 10105–10119.
Vera de la Puente, C.V., 1989. Estratigrafía, sedimentología y paleogeografía de los grupos Rañeces y La Vid en la Cordillera Cantábrica (Asturias y León). Phd Thesis. Universidad de Oviedo, p. 653.
Verrall, P., 1981. Structural interpretation with application with application to North Sea problems. Joint Association of Petroleum Exploration Courses (JAPEC). Course Notes 3.
Waltham, D., 1989. Finite difference modelling of hangingwall deformation. J. Struct. Geol. 11 (4), 433–437.
Watkins, H., Bond, C.E., Cawood, A.J., Cooper, M.A., Warren, M.J., 2020. Fracture distribution on the Swift Reservoir Anticline, Montana: implications for structural and lithological controls on fracture intensity. In: Bond, C.E., Lebit, H.D. (Eds.), Folding and Fracturing of Rocks: 50 Years of Research Since the Seminal Text Book of J. G. Ramsay, 487. Geological Society Special Publications, pp. 209–228.
Weil, A.B., Van der Voo, R., Van der Pluijm, B. A., Parés, J.M., 2000. The formation of an orocline by multiphase deformation: a paleomagnetic investigation of the Cantabria-Asturias Arc (northern Spain). J. Struct. Geol. 22 (6), 735–758.
White, N., Jackson, J.A., McKenzie, D.P., 1986. The relationships between the geometry of normal faults and that of the sedimentary layers in their hanging walls. J. Struct. Geol. 8, 897–909.
Williams, G., Vann, I., 1987. The geometry of listric normal faults and deformation in their hanging walls. J. Struct. Geol. 9, 789–795.
Worrall, D.M., Snelson, S., 1989. Evolution of the northern Gulf of Mexico, with emphasis on Cenozoic growth faulting and the role of salt. In: Bally, A.W., Palmer, A. R. (Eds.), The Geology of North America: an Overview. GSA, Boulder, pp. 97–138.
Xiao, H., Suppe, J., 1992. Origin of rollover. AAPG (Am. Assoc. Pet. Geol.) Bull. 76 (4), 509–529.